Process Safety and Environmental Protection 181 (2024) 294–311

Contents lists available at ScienceDirect

Process Safety and Environmental Protection

journal homepage: www.journals.elsevier.com/process-safety-and-environmental-protection

Assessment of Safety Barrier Performance in Environmentally Critical Facilities: Bridging Conventional Risk Assessment Techniques with Data-Driven Modelling

Nicola Tamascelli [a,b], Alessandro Dal Pozzo [a], Giordano Emrys Scarponi [a], Nicola Paltrinieri [b], Valerio Cozzani [a,*]

[a] LISES - Laboratory of Industrial Safety and Environmental Sustainability, DICAM - Department of Civil, Chemical, Environmental and Materials Engineering, Alma Mater Studiorum – University of Bologna, via Terracini n.28, 40131 Bologna, Italy
[b] Department of Mechanical and Industrial Engineering, NTNU, Trondheim, Norway

ARTICLE INFO

Keywords:
Hazard identification
Safety barriers
Digital model
Dynamic performance assessment
Flue gas treatment
Waste-to-energy

ABSTRACT

The failure of emission control systems in industrial processes undergoing emission regulations can cause severe harm to the environment. In this context, safety engineering principles can be applied to analyze process deviations and identify suitable safety barriers to mitigate harmful emissions during critical events. However, the selection, design, and assessment of proper safety barriers may be complex due to several contingencies such as the inability to perform extensive field tests on systems under strict emission regulations. In this study, an approach is proposed to couple conventional hazard identification techniques with a digital model of a flue gas treatment system to support the identification and performance assessment of safety barriers for emission control. Resilience analysis is used to evaluate the behavior of the most relevant safety barrier options, selected through a screening with conventional hazard identification tools. Barriers are simulated using the digital model of the system, gathering key information for their design and evaluation, and overcoming the limitations to field tests at the real plant. The methodology is illustrated with reference to acid gas removal in waste-to-energy facilities, a relevant example of an emission control system that is typically exposed to significant process deviations.

1. Introduction

Several industrial processes have the potential to cause significant harm to the environment if their routine emissions to air and water are not minimized thanks to the application of proper treatment systems. In analogy with the definition of safety-critical systems in the field of safety engineering (Daintith and Wright, 2008; Knight, 2002; Maurya and Kumar, 2020), these systems can be defined environmentally critical systems, as their failure or malfunction may result in an unacceptable environmental damage.

Environmentally critical systems in the field of emission reduction need to exhibit: i) high performance, often corresponding to > 90% pollutant removal efficiency (e.g. see the Best Available Techniques reference documents of the European IPPC Bureau (European Commission, 2020)), and ii) high availability, according to the continuous operation of the plants on which they are installed.

Flue gas cleaning in waste-to-energy (WtE) plants represents a relevant example of such systems. WtE facilities are subject to some of the more stringent emission standards among industrial sectors (Dal Pozzo et al., 2023c; Van Caneghem et al., 2019) for a variety of pollutants, including nitrogen oxides (NO_X), acid pollutants such as hydrogen chloride (HCl) and sulfur dioxide (SO_2), and trace elements such as mercury (Hg). In Europe continuous emission measurement at stack is prescribed for these pollutants (European Commission, 2020). Therefore, WtE flue gas treatment (FGT) systems have to meet low emission levels in continuous operation, typically in presence of high fluctuations of the pollutant concentrations in the raw flue gas, as a consequence of the wide variety over time of the composition of the waste fed to the plant (Dal Pozzo et al., 2016).

In this context, the system is required to perform adequately during normal operating conditions and/or in the presence of external and internal disturbances. Actually, deviations caused by sudden variations in

* Corresponding author.
E-mail address: valerio.cozzani@unibo.it (V. Cozzani).

https://doi.org/10.1016/j.psep.2023.11.021
Received 20 July 2023; Received in revised form 4 October 2023; Accepted 10 November 2023
Available online 15 November 2023

the composition of the waste feed or by malfunctions in FGT components can lead to a loss of control of pollutant emissions, which may result in exceeding the emission limit values (ELV). Therefore, it is critical to ensure that FGT systems are robust against unwanted events, thus safeguarding WtE systems with respect to the risk of environmental damage deriving from ELVs exceedance. However, specific methodologies aimed at assessing and managing such risk are still missing.

The chemical and process industry has developed and consolidated risk management techniques based on extensive experience in managing hazardous substances and safety-critical operating conditions (Khan et al., 2015). Many of these techniques have become routine in risk management and have been included in standards and guidelines (Delvosalle et al., 2006; International Organization for Standardization, 2019, 2018). Nevertheless, these methods are not specifically conceived to evaluate and improve environmentally critical systems, and their application to such systems is not straightforward. As an example, the conventional approach towards the analysis and assessment of the environmental performance of FGT systems in current industrial practice is highly empirical and is based on extensive test run campaigns at the plant, which have a critical limitation in the aforementioned need for continuous compliance with strict emission limits. Thus, an alternative perspective is required to address the systematic assessment of critical events that may undermine the performance of FGT in WtE systems.

Approaching the study of environmentally critical systems from a process safety standpoint, the loss of control of pollutant emissions may be considered a top event leading to the exceedance of the ELVs, caused by a set of initiating events (e.g., failures of technical systems). A Bow-Tie diagram may be used to represent such critical scenarios (CCPS and Energy Institute, 2018). Bow-tie diagrams are graphical tools including the causes (i.e., initiating events, on the left side of the diagram), the top event (in the center), and the consequences (on the right side of the diagram) of critical scenarios. Physical and non-physical measures intended to mitigate, prevent, or control such critical scenarios may be considered safety barriers (Sklet, 2006) and are usually represented in Bow-Tie Diagrams. A schematic representation of a Bow-Tie diagram is shown in Fig. 1.

Safety barriers play a key role in ensuring the safety of process operations in safety-critical systems (Liu, 2020), thus may have an important role as well in the safe operation of environmentally critical systems. Several studies address the role and performance assessment of safety barriers in safety-critical systems (e.g. see Landucci et al., 2015 and Misuri et al., 2021). However, to the best of the authors' knowledge, there is no attempt to specifically address the estimation of safety barrier performance in environmentally critical systems, such as FGT plants. Actually, the analysis of the relevant literature, further discussed in the following (see Section 2), highlights two substantial gaps concerning safety barrier evaluation in environmentally critical systems. Firstly, there is little (if any) use of well-established risk management techniques derived from other industrial sectors with extensive experience in risk management (e.g., the chemical and process industry). Secondly, the advent of digitalization and digital technologies allows the development of dynamic and inherently updatable models that may be used for assessing the performance of safety barriers. Yet, such models are hardly used in the field of environmental risk management.

In order to address the gaps evidenced above, the present study aims at presenting a specific innovative methodology combining conventional hazard identification techniques with a digital model of a FGT process in order to identify, simulate, and evaluate safety barriers that may prevent or mitigate excessive emissions in case of process deviations. In the proposed methodology, hazard identification approaches are used to screen possible process deviations and identify the most critical scenarios, which are then simulated using the digital model of the system with or without the application of safety barriers considered for installation. Resilience analysis is then performed to obtain a dynamic measure of the barrier performance under different conditions and barrier configurations. The methodology is demonstrated by its application to a representative case study, addressing the acid gas removal in a WtE facility. Although the detailed procedure required for the application of some steps of the methodology is governed by the specific features of the case-study considered, the overall approach and the structure of the methodology have a general validity, allowing its application to other environmentally critical systems, aiming at the assessment of the effectiveness of safety barriers and the performance tuning of scalable safety barriers.

The remainder of this paper is organized as follows. Section 2 outlines the state of the art of safety barrier performance assessment in relation to dynamic risk assessment (DRA) and resilience engineering, which is the starting point of the developed methodology. Section 3 presents the innovative methodology developed, in combination with its application to the case-study. The reference FGT facility used to test the approach is described in Section 4. Results are presented in Section 5 and discussed in Section 6, which also highlights the limitations of the study and provides suggestions for future developments. Finally, conclusions are drawn in Section 7.

2. Safety barrier assessment in the perspective of DRA and resilience engineering

Regardless of the specific field of application, most contributions estimate the performance of a safety barrier based on a set of indicators, such as barrier effectiveness and availability (Sklet, 2006). The effectiveness of a safety barrier represents its "ability to perform a safety function for a duration, in a non-degraded mode and in specified conditions" (De Dianous et al., 2004), while the availability represents the ability to perform its function while needed. Several studies focused on

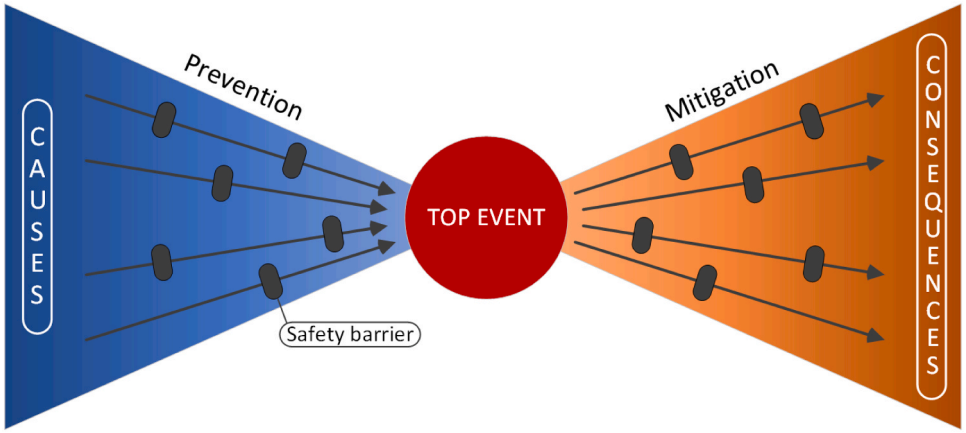

Fig. 1. A Bow-Tie diagram.

estimating the performance of safety barriers (Liu, 2020). For example, Landucci et al. (2015) proposed a method for the quantification of the effectiveness and availability of safety barriers during domino scenarios triggered by fire. The study was further refined by Bucelli et al. (2018) to consider the influence of harsh climate conditions in offshore facilities. Misuri et al. (2021) investigated the impact of Natural Hazards Triggering Technological Accidents (Natech) on barrier performance and proposed a method to modify the Probability of Failure on Demand of safety barriers to account for the effect of natural disasters. However, formal techniques treat safety barriers as static objects, with constant effectiveness and availability values. Such a static perspective cannot capture the dynamic features of the processes involved (e.g., degradation, aging, overlooked hazards). In fact, most canonical methods in risk management are not designed to be easily updatable (Paltrinieri and Khan, 2020), which implies their inability to reflect the evolving real-world risk. The inherently static nature of conventional Risk Assessment methods has been often criticized by academics and practitioners, and is of specific concern in some environmentally critical systems, as WtE, which are inherently exposed to relevant modifications of operating conditions in time. Moreover, the advancements in industrial automation and robotics have increased the complexity and interconnectedness of industrial plants (Villa et al., 2016). In an attempt to overcome these limitations, methods for safety barrier assessment have been directed towards the so-called Dynamic Risk Analysis (DRA), which deals with the development of methods that can provide the update of risk figures considering the variations in the performance of safety-critical systems, such as the control and alarm systems, safety barriers, and maintenance activities (Khan et al., 2016). In the context of DRA, safety barriers are no longer considered static units but dynamic entities, that interact with and are affected by a dynamic environment, and whose performance varies over time due to changes in internal and external conditions (Bubbico et al., 2020). Therefore, DRA aims to define methods and frameworks that are inherently updatable in order to consider new information and capture unsafe operating conditions among highly connected systems. A survey of existing literature indicates that there are only a few DRA methodologies that specifically address the dynamics of safety barriers. For instance, Han et al. (2019) employed Bayesian Networks to model the failure rate of safety barriers. They utilized historical failure data to establish a prior distribution for the barrier failure rate, which was eventually updated as new data emerged. Similarly, Sarvestani et al. (2021) applied Bayesian reasoning to assess the risks associated with LPG accidents. Also, Zeng et al. (2020) employed Bayesian Networks to trace the spatial-temporal progression of fire-related domino effects, integrating the influence of safety barriers directly into the network structure. However, such approaches often necessitate a significant amount of data, in particular concering system failures, for network calibration. Given the infrequent occurrence of such events, obtaining these data is challenging. Furthermore, expert elicitation is commonly used to determine probability distributions, introducing an additional layer of uncertainty.

To the best of the authors' knowledge, there has not been a dedicated study addressing the dynamic evaluation of barrier effectiveness within environmentally critical facilities. In this context, resilience engineering has gained significant importance among safety scientists, motivated by the need to manage risk in increasingly complex systems (Bergström et al., 2015). Similarly to DRA, resilience analysis focuses on capturing risk variability due to component failures, external disturbances, and/or dysfunctional interactions among system components (Leveson et al., 2006). However, resilience puts more emphasis on the intrinsic ability of a system to "adjust its functioning prior to, during, or following changes and disturbances, so that it can sustain required operations under both expected and unexpected conditions" (Hollnagel et al., 2011). That is, resilience engineering approaches system safety from a slightly different perspective, which focuses on how systems absorb sudden disturbances, recover after disruptive events, and adapt to new conditions while maintaining acceptable performance (Yarveisy et al., 2020). Several studies have focused on resilience analysis to address safety of complex socio-technical systems (Patriarca et al., 2018). However, only a few contributions leverage resilience engineering to evaluate the performance of safety barriers (Bai et al., 2022; Sun et al., 2021; Thieme and Utne, 2017). In addition, no study has been proposed to address the safety of environmentally critical systems from a resilience perspective.

DRA and resilience analysis rely on updatable models that can (i) grasp the system dynamics and (ii) consider the effects of unsafe interactions. However, the increasing complexity and interconnectedness of industrial plants prevent the development of rigorous modeling. For example, it is challenging to describe the dynamics of the acid gas neutralization mechanism occurring in an FGT plant through first principles due to the complexity of the phenomena involved (e.g., convection, diffusion in a solid porous media, reaction kinetics, thermodynamic equilibria) and other external and internal factors that are difficult to control and monitor (e.g., thickness and reactivity of the filter cake, the composition of the flue gas, changes in the sorbent structure) (Antonioni et al., 2016; Dal Pozzo et al., 2018b). In this context, the emergence of digitalization in process industry can provide tools and methods to overcome such limitation (Kockmann, 2019). Thanks to the wealth of data typically available from plant sensors and measurement devices, it is possible to derive digital models of the pollutant removal processes of varying degree of complexity that can be used for process optimization purposes. Reliable data-driven models of different operations in the WtE flue gas cleaning can be developed from representative datasets of past performance of the plant (Magnanelli et al., 2020; Pozzo et al., 2018) or compact test protocols (Bacci Di Capaci et al., 2022). Dal Pozzo et al. (2021) demonstrated how the use of a properly calibrated digital model reproducing the behavior of a real FGT system enables an extensive testing of alternative control strategies in a virtual environment. The final application of the optimized control strategy tuned via the digital model to the real plant showed a significant reduction compared to the default control logic of the plant. The approach allowed to achieve such process control optimization with a minimal need for test runs at the real plant.

Therefore, based on the above analysis of the relevant literature, the method developed in the present study introduces a dynamic evaluation of the barrier performance, allowing its update based on new data and knowledge becoming available during process operation. Moreover, a specific approach based on a digital model of the FGT system is developed to allow testing the limits of system performance in a virtual environment, limiting the use of full-scale test-runs that may lead to hazardous conditions when approaching critical emission values. Finally, resilience analysis is applied to obtain a dynamic measure of the barrier performance.

3. Methodology

The approach proposed in this study is composed of six steps, which are outlined in Fig. 2 together with their inputs and outputs. The methodology relies on the integration between advanced risk management tools (e.g., hazard identification techniques) and innovative modeling methods (e.g., data-driven regression models). The former are used to define a set of critical scenarios and additional safety barriers that may prevent or mitigate such critical events. The latter allow the simulation of critical scenarios and of safety barrier performance without the need for field tests or first principles models. A detailed description of each step included in the methodology is given in the following. For the sake of clarity, the specific steps of the methodology addressing digital model development and safety barrier modeling are developed addressing the features of FGT systems in WtE, for which a case-study will be discussed in the following.

3.1. Process layout definition and data collection

In this step, relevant information on the process considered must be

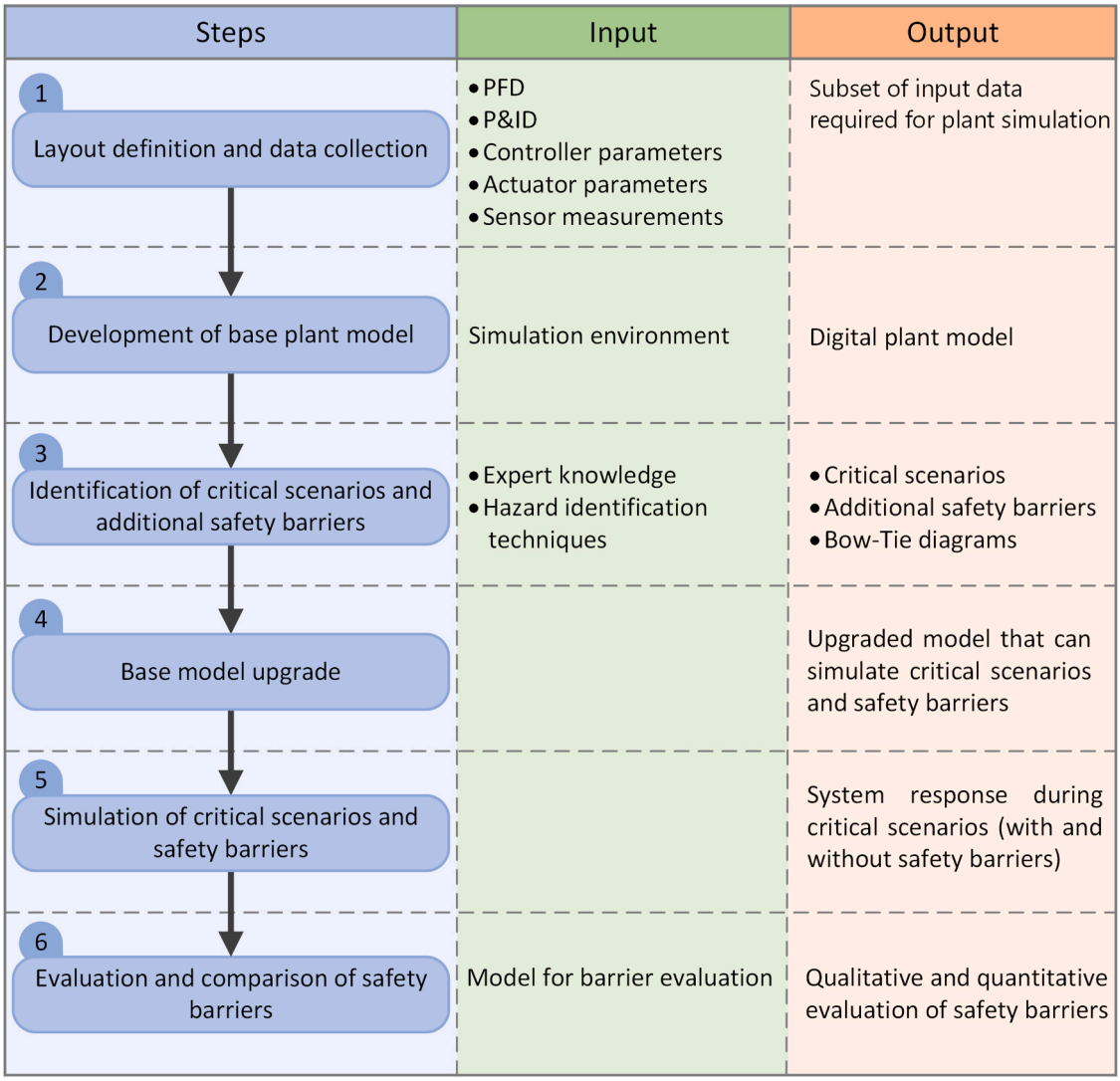

Fig. 2. Overview of the methodology.

collected and stored. The minimum set of data includes the following:

1. Process Flow Diagrams (PFD) and Piping and Instrumentation Diagrams (P&ID);
2. Parameters of the control loops;
3. Process data collected during different operating conditions.

PFD and P&ID are required to determine the process layout and the control strategy.

When considering a typical FGT section, this includes filters (i.e., fabric filters or electrostatic precipitators), reactors (e.g., spray driers, scrubbers, in-line reactors), injection devices (e.g., screw feeders), and measurement devices (e.g., thermocouples, flow meters, gas analyzers). An overview of the most used techniques for the reduction of acid gases is reported in Section 2.5.4 of the Best Available Techniques (BAT) Reference Document for Waste Incineration (European Commission, 2019).

In addition, it is critical to determine the control strategy adopted to regulate the injection of sorbent (e.g., feedback, feedforward, mixed hybrid control strategies). After the identification of the control strategies, the design parameters of controllers and actuators must be collected. That is, input-output models or, alternatively, transfer functions of controllers and actuators must be defined in terms of mathematical structure and parameters. This information may be provided by the plant personnel or may be available in technical manuals.

Finally, process data from various operating conditions must be collected and stored. These data are required to build the data-driven model of the acid gas reduction mechanism. Therefore, it is critical to ensure that data are closely related to the reaction dynamics. With reference to Fig. 3, representing a general scheme of a FGT, the minimum set of process data may include:

- The concentration of acid gases in the flue gas entering the system (stream number 1 Fig. 3), namely $C_{acid,in}$.
- The concentration of acid gases in the clean gas leaving the system (stream number 3 in Fig. 3), namely $C_{acid,out}$.
- The mass flow rate of the sorbent (stream number 2 in Fig. 3), namely $\dot{m}_{sorbent}$.

Data come in the form of time series representing the evolution of process variables with time and may be stored in a matrix-like database D, whose columns represent process variables and rows indicate time instants.

It is worth mentioning that the type and number of process variables available for collection and the total amount of observations largely depend on the specific application. Actually, different plants have different sensors and measuring points. However, the process variables mentioned above should be easy to obtain in most facilities (directly or

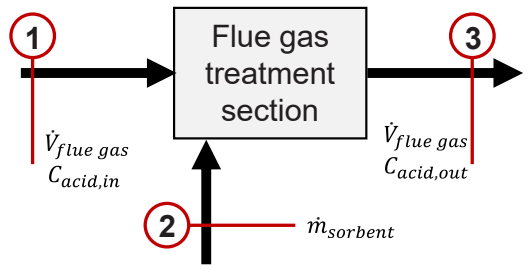

Fig. 3. General schematization of a flue gas treatment section for acid gas removal.

derived from other measured variables).

The data collection process aims to capture the plant behavior during various operative conditions, including normal operations, disturbances, and malfunctions. Thus, the dataset D should encompass a wide range of values for the process variables, maximizing information content. It is thus crucial to adequately capture the variability and diversity of the process conditions to enable an accurate and robust model development. Sufficiently representative time-series should be available, in the range of weeks up to month, depending on the features of the plant. Actually, most distributed control systems nowadays store long time series of process data (up to several years), thus providing sufficient information for the implementation of the method.

Furthermore, process data should be sufficiently granular to allow a thorough investigation of the dynamics involved in the processes. An adequate level of granularity is essential to capture accurately the intricate temporal variations and interactions within the system. A minimum granularity, in terms of sampling time, of 1 min is usually adequate to ensure that the data capture the necessary temporal resolution, enabling a detailed analysis of the processes' dynamics and facilitating accurate modeling.

3.2. Development of a base plant model

The base plant model ($\mathscr{M}$) is a digital model of system of concern. In the present study, the FGT section of a WtE was considered. The purpose of the model is to mimic the plant dynamics in terms of (i) control logic and actuators and (ii) acid gas reduction. In other words, the model takes as an input the concentration of acid gases in the flue gas at time t (i.e., $C_{acid,in}(t)$), and returns the concentration of acidic compounds in the clean gas at time $t+1$ (i.e., $C_{acid,out}(t+1)$):

$$C_{acid,out}(t+1) = \mathscr{M}\left(C_{acid,in}(t)\right) \tag{1}$$

The digital model comprises several sub-models that mimic a specific plant function. For example, there may be sub-models to replicate the controller behavior, measuring instruments, the reaction dynamics, and so forth. The number and nature of the sub-models largely depend on the specific plant under consideration. The analysis of PFDs and P&IDs is essential to define the structure of $\mathscr{M}$. In most plants, the digital model comprises at least three sub-models:

- The sub-model g that mimics the actuator;
- The sub-model f that mimics the controller action;
- The sub-model h that mimics the reaction dynamics.

In this case, Eq. (1) may be written as follows.

$$C_{acid,out}(t+1) = h\left(g(f(t)), C_{acid,in}(t)\right) \tag{2}$$

Where $f(t)$ represents the controller signal at time t, and $g(f(t))$ indicates the manipulated variable at time t (e.g., $\dot{m}_{sorbent}(t)$).

Data collected in step 1 of Fig. 2 allow the rigorous modeling of actuators and controllers. However, modeling the reaction dynamics through first principles is challenging. A viable solution to model the reaction mechanism is to rely on data-driven methods. Here, the idea is to leverage plant data collected in step 1 in Fig. 2 to build a data-driven model of the acid gas reduction mechanism. This model may take as an input (i) the concentration of acid gases entering the system and (ii) the sorbent flow rate, and return the concentration of acidic compounds in the clean gas leaving the system.

The problem described in Eq. (2) belongs to the vast area of time-series forecasting (Box et al., 2015). Therefore, h may be considered a regression model that takes a set of observations as an input and returns the value of a target variable. The selection of the model h is a critical step to ensure adequate performance (Emmert-Streib and Dehmer, 2019). However, a complete overview of available models and model selection techniques is unfeasible considering the vastity of the topic. The reader might refer to the literature on system identification (Ljung, 2010, 1999) and data mining (Kotu and Deshpande, 2019; Torres et al., 2020) to explore different modeling strategies.

Regardless of the specific model, the development of h involves at least two steps: training and evaluation. Firstly, the dataset D (i.e., process data collected in step 1 of Fig. 2) is split into two parts, namely D_t and D_e, such that $D = \begin{vmatrix} D_t \\ D_e \end{vmatrix}$. D_t is used to train the model while D_e is used in the evaluation phase. Typically, D_t contains 80% of the observations in D. Also, D_t may be conceptually divided into two parts. The first part (X_t) comprises the inputs of the model (i.e., $C_{acid,in}(t)$ and $\dot{m}_{sorbent}$), the second part (Y_t) comprises the variable that must be predicted (i.e., $C_{acid,out}(t+1)$), such that $D_t = |X_t\ Y_t|$. The same applies to D_e.

Secondly, the model is trained. Training involves the optimization of the model's internal parameters (θ) to minimize a loss function $(\mathscr{L})$.

$$\widehat{\theta} = \underset{\theta}{argmin}[\mathscr{L}(\theta, D_{train})] \tag{3}$$

Where $\widehat{\theta}$ represents the optimized model's parameters. Some widely used loss functions include the Sum of Squared Residuals (SSR), the Mean Squared Error (MSE), Mean Absolute Error (MAE), Hubert Loss, and Log-cosh loss (Wang et al., 2022). As an example, if SSR is used, the loss function is:

$$\mathscr{L}(\theta, D_{train}) = \sum_{i=1}^{N} (y_t(t+1) - h(x_t(t), \theta))^2 \tag{4}$$

Where $y_t(t+1) \epsilon Y_t$, N represents the number of observations in D_t, and $x_t(t) \in X_t$.

After training, the performance of the model must be evaluated using a new set of data. To this end, the model is used to perform predictions on the observations included in D_e. Eventually, performance indicators are calculated to quantify the prediction performance. For example, the Root Mean Squared Error (RMSE) may be calculated as follows:

$$RMSE = \sqrt{\frac{1}{M}\sum_{i=1}^{M} (y_e(t+1) - h(x_e(t), \widehat{\theta}))^2} \tag{5}$$

Where, $y_e(t+1) \epsilon Y_e$, M represents the number of observations in D_e, and $x_e(t) \in X_e$.

A user-defined acceptance criterion may be defined to discriminate between acceptable and non-acceptable performance. For example, if the RMSE is smaller than a threshold, the model h may be considered adequate to simulate the reaction dynamics.

It is worth mentioning that the procedure described above is intended to be a quick overview of the steps required to train and evaluate the model. It is not meant to be the best strategy. For example, the so-called holdout method is described above to keep the description short. The reader may adopt more advanced evaluation methods, such as holdout with validation or cross-validation (Raschka, 2018). Also, Eq. (2) assumes that the input to the data-driven model are inlet concentration of acid gases and sorbent mass flow rate. Nevertheless, the method may be promptly adapted to consider more input data, such as the flue gas temperature, the flue gas volumetric flow rate, the pressure drop across

the filters, and so forth.

3.3. Identification of critical scenarios and additional safety barriers

The FGT section is analyzed to identify (i) critical scenarios and (ii) recommendations for additional safety barriers. In this context, critical scenarios are events that have the potential to cause a significant increase in the acid gas concentration downstream of the treatment section. In other words, the analysis aims at answering the following questions:

1. Which critical events have the potential to cause a significant increase in acidic compounds in the clean gas leaving the treatment section (stream 3 in Fig. 3)?
2. Which additional safety barriers may prevent or mitigate critical events?

Traditional hazard identification techniques, such as HazOp, HazId, analysis of historical data, what-if analysis, and brainstorming (Mannan, 2005), may be used to answer these questions. Data collected in step 1 in Fig. 2 (e.g., PFD, P&ID) and the operational experience of plant personnel are the starting point of the analysis.

The selection of the actual hazard identification technique to be applied is guided by several factors, such as time constraints, objectives of the analysis, and the required level of detail (International Organization for Standardization, 2019; Mannan, 2005). Structured techniques (e.g., HazOp) provide more information and a deeper understanding of the hazards. On the other hand, unstructured methods (e.g., brainstorming) are faster and cheaper, but a higher level of expertise may be required to ensure the quality and completeness of results.

Often, the combined use of multiple hazard identification techniques leads to a more comprehensive risk identification (International Organization for Standardization, 2019). However, regardless of the specific techniques adopted, the results of the analysis should provide:

- A list of critical events, along with their causes and consequences on acid gas emission at stack;
- A list of recommended safety barriers.

Results may be condensed in a bow-tie diagram to provide a concise visual representation of critical events and safety barriers (CCPS and Energy Institute, 2018). The top event may be formulated as a “significant increase in the acidic compound concentration in the clean gas”. Among the end-point events on the right-end part of the diagram (consequences) specific possible outcomes of the top event should be listed (e.g., “half-hourly emission limit values exceeded”), while the leftmost part shows the causes of the top event. Recommended safety barriers should be included in the bow-tie to clarify their role in preventing or mitigating the critical event.

3.4. Base model upgrade

The base plant model developed in step 2 of Fig. 2 is designed to mimic the plant response during normal operating conditions. Therefore, modifications may be needed to simulate the effect of critical events and additional safety barriers identified (step 3 in Fig. 2).

Depending on the nature and extent of modifications, there are two viable solutions to update the base plant model. These include:

1. First principles modeling;
2. Data-driven modeling using data from test-runs.

If the modifications are associated with well-known systems where first principle models are available, it is possible to employ rigorous modeling techniques to incorporate the behavior of critical events and safety barriers. For example, if a critical event involves the failure of a control loop, the equations governing the controller can be modified to account for the faulty behavior.

However, when the effect of critical events and additional safety barriers is uncertain and cannot be accurately described using rigorous models, data-driven methods may be used. Data from different facilities that have experienced similar failures or implemented similar safety barriers may be used to this aim. Clearly enough, if limited data are available, carrying out specific test runs on pilot facilities or on the actual plant may be considered as an alternative in case the safe operation of the system may be granted. The reader is referred to previous studies (Bacci Di Capaci et al., 2022; Dal Pozzo et al., 2021) for details and discussion on the design of data collection campaigns for WtE flue gas cleaning systems.

Regardless of the particular updating procedure, the simulation of critical events and safety barriers necessitates the modification of existing sub-models or the development of new sub-models. This process enables the creation of an upgraded model, denoted as $\mathscr{M}''$, that can (i) simulate the effect of the critical events on the original gas treatment system and (ii) simulate the system response after the installation of all (or part of) the recommended safety barriers.

3.5. Simulation of critical scenarios and safety barriers

The upgraded model $\mathscr{M}''$ is used to simulate the critical events identified in step 3 of the methodology (see step 5 in Fig. 2). Two distinct simulation runs are performed.

The first run aims at evaluating the response of the original gas treatment system during critical scenarios. That is, all the barrier sub-models are excluded in this first run of simulations. In this phase, each critical event identified in step 3 of Fig. 2 is simulated to obtain the trends of $C_{acid,out}(t)$ and $\dot{m}_{sorbent}(t)$, describing the original plant response in the presence of critical disturbances. This first set of simulations is used as a benchmark to evaluate the improvements due to the implementation of the additional safety barriers.

The second group of simulations focuses on the system response after the installation of the safety barriers identified in step 3 of the procedure (see Fig. 2). To this end, the bow-ties produced are analyzed to identify relevant safety barriers for each critical event considered. Safety barriers are selected based on their ability to affect the operation of the specific critical event under consideration. As a result, a set of safety barriers is selected for each critical event. The upgraded plant model is then used to simulate the effect of safety barriers considering that only part of the barriers may be active during a critical event. That is, if a critical event is associated with a set of N safety barriers, the number of simulations required is $2^N - 1$. In each simulation, the model returns $C_{acid,out}(t)$ and $\dot{m}_{sorbent}(t)$, which are used to quantify the improvements due to the implementation of the safety barriers.

3.6. Evaluation and comparison of safety barriers

The output of the simulations provides a dynamic picture of the system behavior with different barrier configurations and during various critical events. These results can be used to evaluate the effectiveness of safety barriers, in both absolute and relative terms. In this context, the general definition of effectiveness introduced in Section 2 has to be declined for the specific problem of emission control as the ability of a safety barrier to ensure that the system complies with ELV. A set of indicators is built to evaluate the barrier effectiveness and allow for a quantitative comparison of alternatives. Resilience analysis is used to quantify the ability of the system to withstand external disturbances and to evaluate the improvements resulting from the installation of additional safety barriers.

Following the generic definition of resilience provided by Hollnagel et al. (2010), the resilience of the gas treatment system may be defined as its ability to fulfill its purpose in a variety of adverse conditions. In the

specific context of acid gas removal, the *purpose* of the system is to comply with ELV, and the *adverse conditions* refer to the critical scenarios identified in step 3 of the method (see Fig. 2).

The literature offers many examples of quantitative resilience metrics (Hosseini et al., 2016). Most of them rely on a time-dependent function $\varphi(t)$ that reflects the performance of the system. This performance function (also called quality function) ranges between zero and one. The performance is zero if the system is in a completely degraded state or, in other words, if it cannot fulfill its purpose. On the contrary, if the system performs as expected, the performance is one.

After a critical event, the system performance degrades, reaches a minimum, and eventually increases as mitigative actions restore normal operations, as exemplified in Fig. 4.

The mathematical formulation of the performance metric depends on the problem under assessment. The performance of the treatment system with respect to the acid compound i (i.e., $\varphi_i(t)$) may be a user-defined function that satisfies the following requirements:

- $\varphi_i(t) = 0$ if the half-hourly concentration of i exceeds the ELV;
- $\varphi_i(t) = 1$ if the absolute deviation between the half-hourly concentration of i and the controller setpoint does not exceed 10%.

The user can choose the type of function expressing the performance based on the problem requirements. The criteria for the selection of performance functions are discussed extensively elsewhere (Hosseini et al., 2016; Tran et al., 2017). In the case-study introduced in the following, an exponential function was used to penalize large deviations from the controller setpoint (see Section 4).

Given the performance, the so-called Resilience Loss (RL) can be used to quantify the loss of resilience caused by a critical event.

$$RL_i = \int_{t_e}^{t_f} [1 - \varphi_i(t)]\,dt \tag{6}$$

Where RL_i indicates the Resilience Loss with respect to the acidic compound i, t_e represents the time of occurrence of the critical event, and t_f is the recovery time, as indicated in Fig. 4. The Resilience Loss ranges between zero and $(t_f - t_e)$. Values close to zero indicate that the system has not been significantly affected by the critical event.

A performance function and a Resilience Loss can be calculated for each acid gas considered and each combination of critical scenarios and safety barriers. The performance metric $\varphi_i(t)$ reflects the system dynamics during the critical scenarios, while RL represents a quantitative indicator that reflects the system capacity to withstand internal or external disturbances. The comparison of $\varphi_i(t)$ and RL_i among alternative configurations and to the benchmark simulations allows a quantitative comparison between alternative process configurations and the identification of the best-performing safety barriers.

It is worth mentioning that other relevant features of the safety barriers, namely their availability and level of confidence, which are related to the reliability and availability of mechanical components and not to their process performance, are considered out of scope of the present analysis.

4. Case study

A full-scale case study was defined to demonstrate the application of the methodology and the potential use of the results obtained. The case study concerns an acid gas removal stage of the FGT section of Municipal Solid Waste Incinerator located in northern Italy.

In WtE operation, the concentrations of hydrogen chloride (HCl) are typically higher of at least an order of magnitude than those of SO_2 and HF (Dal Pozzo et al., 2023a). Hence, for the sake of simplicity, in the case-study only HCl removal will be considered, since in the current practice fulfilling the ELV of HCl is more critical.

A process flow diagram of the specific FGT system considered in the case-study is reported in Fig. 5. As shown in the Fig. 5, the flue gas (stream 1 in Fig. 5) enters an entrained flow-reactor where a solid sorbent (hydrated lime - stream 9) is injected into the flue gas. The entrained-flow stream of gas and solids (stream 2) enters the bag filter F-01, where solids (stream 4) are removed from the clean gas (stream 3). HCl in the gas stream is neutralized according to the following reaction:

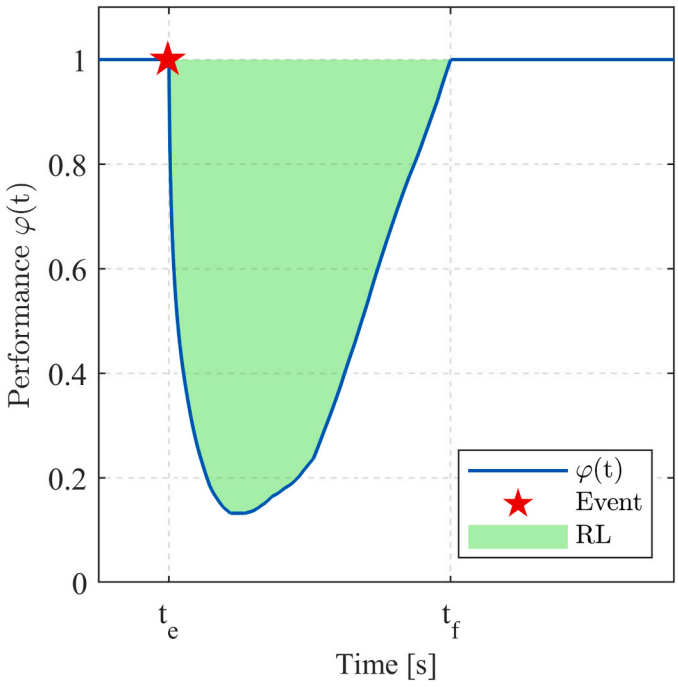

Fig. 4. Typical behavior of the FGT system following a critical event.

$$2HCl + Ca(OH)_2 \leftrightarrow CaCl_2 + 2H_2O \tag{7}$$

The gas-solid reaction takes place in the entrained flow reactor (R-01) and in the cake formed on the filter bags (F-01).

The sorbent mass flow rate is controlled by means of a simple feedback control loop. Specifically, a PI controller (AIC 02) is used to regulate the speed of the feeder motors (M) based on the concentration of acidic compounds in the clean gas leaving the system (stream 3). Two screw feeders are installed in parallel. During normal operations, only one of the two screw feeders operates (T-01), while the other is used as a backup during maintenance or in case of failure of the main feeder. Low-speed alarms (SAL) are installed to detect a blockage or failure of the feeder, allowing a swift start-up of the backup feeder by the control room operator. The configuration shown in Fig. 5 is among the solutions most frequently installed for acid gas removal in European incinerators according to recent surveys (Beylot et al., 2018; Dal Pozzo et al., 2018a) and is listed among the BAT for acid gas treatment (European Commission, 2020). Thus, the case-study introduced is highly representative of the current industrial practice.

The methodology outlined in Section 3 was applied to the analysis of the case study. First, the relevant documentation concerning the selected facility was collected, as indicated in step 1 of the methodology (see Fig. 2). Specifically, the plant personnel provided PFDs, P&IDs, Operating and Control Philosophy, and details on the controller and actuator parameters. Furthermore, a data collection campaign was designed and performed to extract relevant process data from the plant Distributed Control System (DCS). In particular, the following process variables were collected with a sampling interval of 30 s:

- Volumetric flow rate, temperature, and HCl concentration of the flue gas from the furnace (stream 1 in Fig. 5);

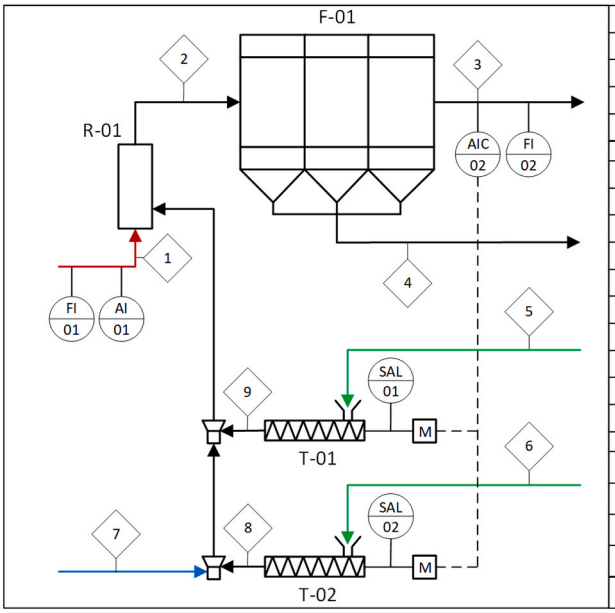

Equipment	Description
R-01	Reactor
F-01	Bag filter
T-01	Main screw feeder
T-02	Backup screw feeder
Stream	**Description**
1	Flue gas from the furnace
2	Gas-solid stream (flue gas and sorbent)
3	Clean gas
4	Solid waste
5	Sorbent feed ($Ca(OH)_2$)
6	Sorbent feed ($Ca(OH)_2$)
7	Compressed air
8	Injected sorbent
9	Injected sorbent
Instrumentation	**Description**
FI	Flow indicator
AI	Composition indicator
AIC	Composition controller
SAL	Slow speed alarm

Fig. 5. Process Flow Diagram of the FGT system for acid gas removal considered in the case-study. Red, green, and blue streams respectively indicate the flue gas entering the FGT section, the sorbent feed, and the compressed air used to inject the sorbent.

- Volumetric flow rate, temperature, and HCl concentration of the clean gas (stream 3 in Fig. 5);
- Mass flow rate of the sorbent (stream 9 in Fig. 5).

A total of four days of observations were collected and stored in tabular format. The collected data were selected to maximize the information stored in data, ensuring the adequacy and significance of the collected data. Matlab Simulink was used to develop the base plant model. Fig. 6 shows the model structure as it appears in the simulation environment. Specific sub-models were developed for each of the equipment items present in the process flow diagram of the plant section considered, shown in Fig. 5.

The input to the base plant model is the molar flow rate of HCl entering the gas treatment system (stream 1 in Fig. 6). The "DCS" block mimics the controller behavior (i.e., AIC-02 in Fig. 5), returning the controller command (signal 2 in Fig. 6) based on the outlet HCl concentration (signal 5 in Fig. 6). The "Screw feeder" block mimics the actuator behavior. It converts the command from the controller into the sorbent mass feed rate injected in the reactor (stream 3 in Fig. 6). Finally, the "Reaction" block represents the data-driven model of the acid neutralization mechanism. Specifically, the model used in this study is a linear Autoregressive with Extra Input model (ARX). The "Reaction" block takes as an input the sorbent feed rate and the molar flow rate of HCl in the flue gas (stream 1 in Fig. 6), and returns the molar flow rate of HCl in the clean gas (stream 4 in Fig. 6), which is eventually converted into the concentration of HCl leaving the system (signal 5 in Fig. 6). Further details on the base plant model used in this study are reported elsewhere (Dal Pozzo et al., 2021).

HazOp analysis has been used to identify critical events that may lead to a significant increase in HCl emissions and the safeguards and/or safety barriers to be installed.

Although the list of critical events identified through the HazOp represents a detailed description of the potential hazards present in the system, some of them may not be credible or may have a marginal impact on HCl emissions. Provided that quantitative information on the causal analysis of FGT systems failure is unavailable in the open literature, an expert elicitation procedure was adopted to complement the HazOp analysis and validate the most relevant process deviations. Expert surveys have been recognized in literature as a relevant tool for a preliminary semi-quantitative evaluation of hazards and related safety barriers (Argenti et al., 2017; Hokstada et al., 1998; Misuri et al., 2020). An ad-hoc survey was prepared and administered to a group of experts with heterogeneous and relevant backgrounds (WtE plant operators, technology suppliers, consultants, academics) that were invited to

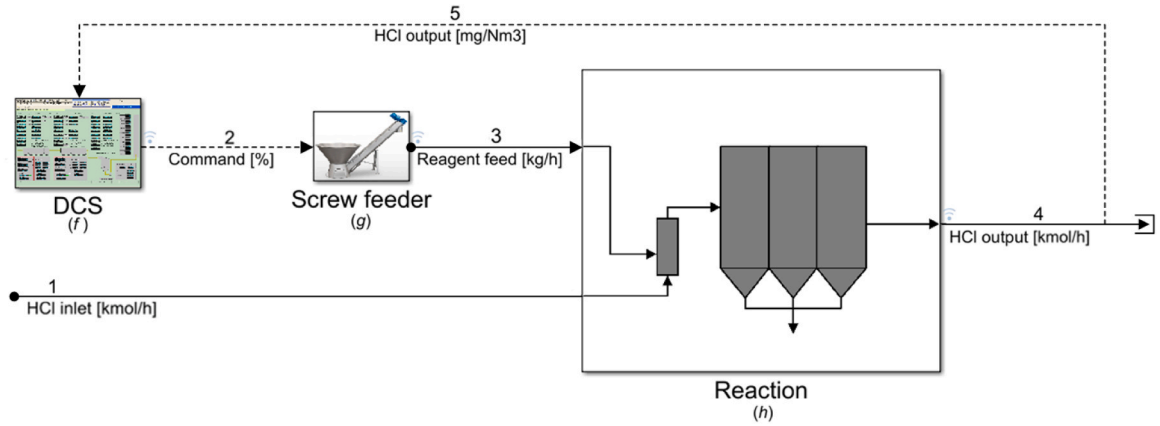

Fig. 6. Translation of the reference FGT system in Fig. 5 into the simulation environment. Items *h*, *g*, and *f* respectively indicate the submodels that mimic the reaction mechanism, the screw feeders, and the control logic. Dashed lines indicate signals and continuous lines represent process streams.

participate anonymously. Considering the specific process scheme in Fig. 5, the experts were asked about the likelihood that given process deviations could trigger a loss of control event, resulting in a temporary overrun of the emission setpoint at stack (sufficient or not to exceed the half-hour emission limit value for the plant). Next, they were asked about the likelihood that given prevention or mitigation measures could avoid such loss of control events. The experts were able to express their answers on a scale 1–5, corresponding to a verbal scale of likelihoods of occurrence from "Extremely unlikely" (i.e., 1) to "(Virtually) certain" (i.e., 5). The transcription of the questionnaire, along with general data collected on the background of survey participants, are reported in the Supplementary Material. The results of the survey supported the identification of the critical scenarios and safety barriers considered for implementation, as discussed in Section 3.3.

Following the identification of critical scenarios and safety barriers, the base plant model was upgraded (step 4 in Fig. 2), and simulations were performed to evaluate the system response with and without the recommended safety barriers (step 5 in Fig. 2). Specifically, two sets of simulations were executed utilizing the upgraded plant model. The first set of simulations models the behavior of the original FGT system during critical scenarios in the absence of any additional safety barriers. The second set of simulations replicates the system response to critical events after the installation of safety barriers. At the end of each simulation, the upgraded plant model returns $C_{HCl,out}(t)$ the concentration of HCl in the clean gas leaving the plant during different critical events and under different system configurations (i.e., with or without safety barriers).

After the simulations, the results were analyzed to evaluate the consequences of the critical events and the benefits derived from the installation of safety barriers. Specifically, the following performance metric was used to assess the performance of the system selected for the case-study:

$$\varphi_{HCl} = \begin{cases} 1 & if\ \overline{C}_{HCl,out}(t) \leq 7.15\ mg_{HCl}/Nm^3 \\ A \bullet exp\left(-B \bullet \overline{C}_{HCl,out}(t)\right) & if\ \overline{C}_{HCl,out}(t) > 7.15\ mg_{HCl}/Nm^3 \end{cases} \quad (8)$$

Where $\overline{C}_{HCl,out}(t)$ indicates the half-hourly HCl concentration at stack at time t, and 7.15 mg_{HCl}/Nm^3 represents the controller setpoint increased by 10% to allow a limited oscillation of the controlled variable. The parameters A and B have been estimated through least squares minimization with the following boundary conditions: $\varphi(7.15) = 1$ and $\varphi(10) = 0$, where 10 mg_{HCl}/Nm^3 represents the ELV. The fitting procedure leads to $A = 3.360 \bullet 10^7$ and $B = 2.424$, which implies $\varphi(10) = 1 \bullet 10^{-3}$. The formulation of the performance metric was inspired by the understanding that the system ability to sustain external disturbances diminishes quickly as the concentration of HCl approaches the ELV. Therefore, the performance metric is designed to degrade exponentially after $\overline{C}_{HCl,out}(t)$ exceeds the allowed level of oscillations and to approach 0 when $\overline{C}_{HCl,out}(t)$ reaches the ELV.

Based on the above defined performance function, the resilience was calculated for each simulated scenario using Eq. (6), enabling quantitative assessment and comparison of safety barriers.

5. Results

In the following, the application of the methodology outlined in Section 3 to the case study introduced in Section 4 is illustrated.

5.1. Critical scenarios and safety barriers

The results of HazOp analysis, used to identify critical events that may lead to a significant increase in HCl emissions and the safeguards and/or safety barriers to be installed, have been condensed into a bow-tie diagram, which is shown in Fig. 7. It is worth mentioning that the bow-tie has been simplified for visualization purposes. The complete bow tie is reported in Figure A1.

The results of the expert survey are shown in Fig. 8. Specifically, Fig. 8.a reports the results related to the credibility of the critical events identified by the HazOp.

It should be remarked that the interviewees generally considered resilient the system in Fig. 5, as only three process deviations (inlet HCl spike +200%, critical waste composition, and clogging of reactant transport line) were deemed likely to cause a temporary overrun of emission setpoint, and only a single deviation (clogging of reactant transport line) was considered likely to cause an overrun severe enough to exceed the half-hour ELV. Among process deviations related to inlet flue gas composition, spikes of HCl were considered significantly more likely. This finding is in agreement with the high HCl to SO_2 ratio typically found in waste-to-energy flue gases (Dal Pozzo et al., 2016) and supports the assumption to consider only HCl in the assessment (see Section 4). The clogging of the reactant transport line was considered the most critical process deviation, followed by failure/blockage of the screw feeder. However, it is worth noticing that an obstruction of the screw feeder was identified by the experts as the most frequent failure experienced in these systems (see section S2 of the Supplementary Material).

Combining the information coming from the HazOp analysis and the expert survey, two critical scenarios were selected for the analysis:

- Critical scenario 1: spike in inlet HCl concentration;
- Critical scenario 2: failure of the screw feeder for reactant delivery.

The survey allowed gathering information also on the effectiveness of possible safety barriers in the critical loss of control of acid gas emission scenarios discussed above. As shown in Fig. 8, the experts were

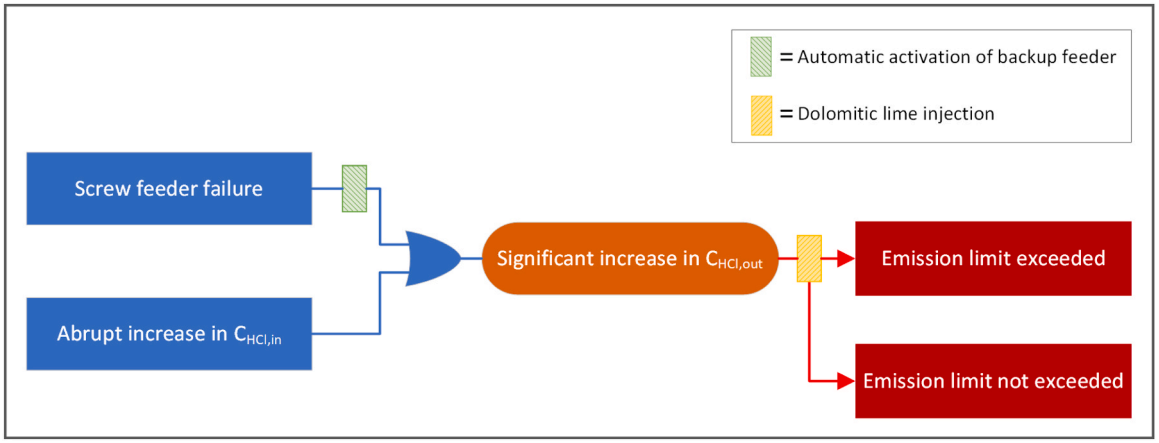

Fig. 7. Simplified bow-tie diagram of the reference FGT system considered in the case-study.

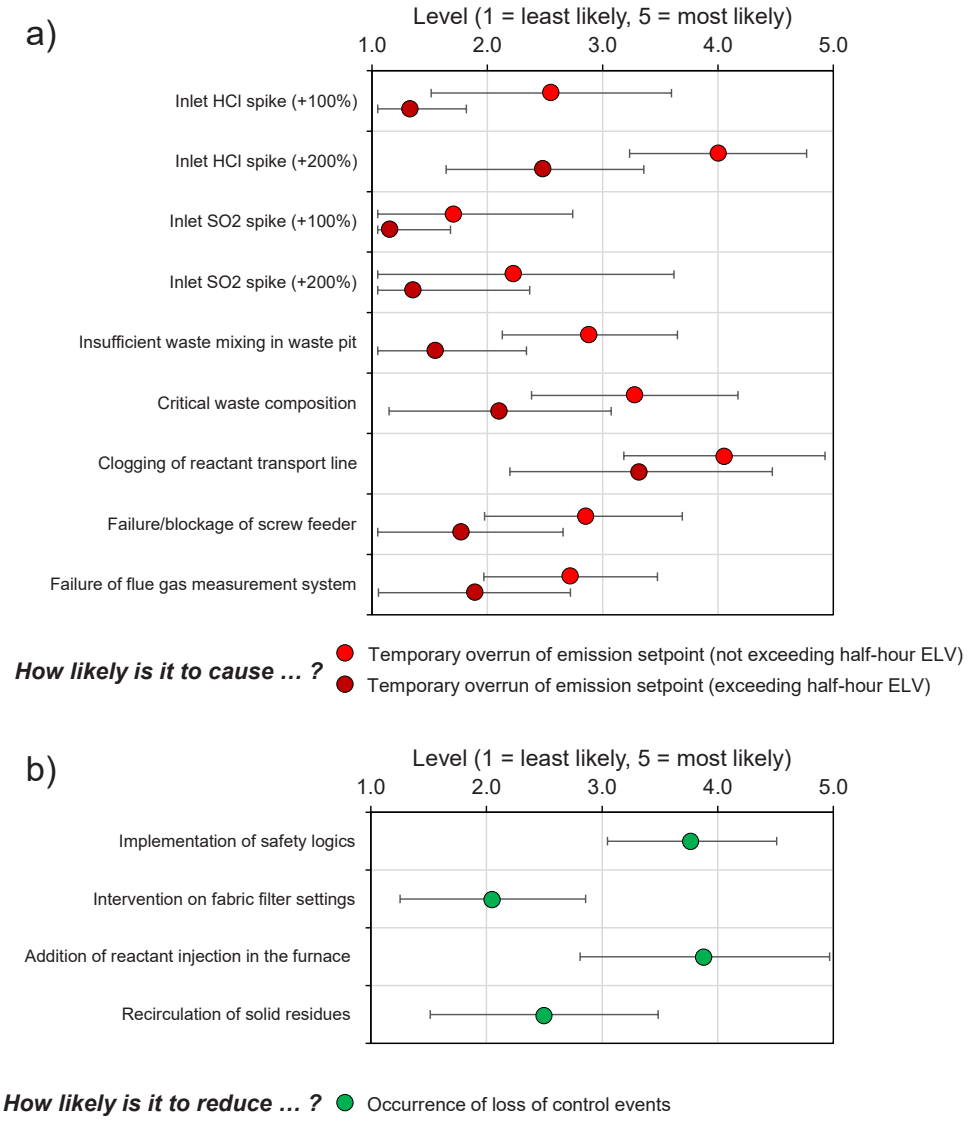

Fig. 8. Results obtained from the expert survey concerning: a) the likelihood of the critical process deviations identified by HazOp to generate loss of control events; b) the likelihood of the listed safety barriers to mitigate loss of control events. Numerical scale (1−5) to be interpreted as in section S2 of the Supplementary Material.

Table 1
List of the safety barrier types considered in the survey.

Type of safety barrier	Description
Intervention on fabric filter settings	Increase of the maximum allowable pressure drop at the fabric filter. **Effect:** *fabric filter cleaning is stopped, allowing longer residence time of the reactant on filter bags and a temporary increase of reactivity in the system.*
Recirculation of solid residues	Re-injection upstream of the fabric filter of part of the process residues collected by the filter. **Effect:** *solid process residues, partially unreacted, which are normally sent to disposal, are recirculated, increasing the overall sorbent-to-acid gas ratio in the system.*
Implementation of safety logics	Implementation of improved safety logics and backup safety systems (e.g., safety logics activating start-up of backup elements). **Effect:** *failure of any element in the control loop triggers the intervention of a backup system that maintain the required feed rate of sorbent:* e.g., *automatic activation of backup sorbent feeders in case of fault of the primary feed control loop.*
Addition of reactant injection in the furnace	Pre-treatment of flue gas in an additional reaction stage upstream of the existing FGT system. **Effect:** *reactant injection in an additional injection point upstream of the FGT system is activated, curtailing spikes of acid gases coming from the combustion chamber before they enter the FGT system.*

asked to evaluate a set of safety barriers, assessing their likelihood to reduce the occurrence of loss of control events and to reduce the consumption of reactant required to mitigate such events. The safety barriers considered in the survey are listed in Table 1.

The first two safety barriers in Table 1 share the common rationale of increasing the residence time of the solid reactant in the system, hence inducing higher solid conversion and increasing HCl removal at equal reactant consumption (Chibante et al., 2010). Although these interventions can help avoiding an excessive consumption of reactants in the control of HCl emissions, the experts consider these systems scarcely effective in reducing the frequency of loss of control events.

Higher scores in terms of likelihood to reduce the occurrence of loss of control events were given to measures that increase redundancy in the FGT system: addition of a pre-treatment HCl removal stage in the furnace (mean score 3.9), and implementation of safety logics (mean score 3.8). The former class of measures is aimed at controlling the effects of high acid gas loads from waste combustion (e.g., critical scenario 1 identified in Section 5.1), while the latter is mainly focused on mitigating the effects of failures of system components (e.g., critical scenario 2 identified in Section 5.1). Therefore, a safety barrier for each of the two classes of interventions was selected as an example for the simulation.

In the case of critical scenario 1, HCl peaks from waste combustion can effectively be mitigated by furnace sorbent injection (Biganzoli et al., 2015). The injection of dolomitic lime in the furnace, a widely applied retrofit solution to improve FGT performance (Dal Pozzo et al., 2023b), was considered for application.

In the case of critical scenario 2, the installation of a safety logic for the automatic activation of the backup feeder by a low-speed alarm was considered to mitigate the possible failure of the main screw feeder of the solid sorbent. It was assumed that such configuration can activate the backup screw feeder in 15 s, compared to at least 5 min in case of a manual intervention by plant operators, which is considered as the base case.

5.2. Base model upgrade

As discussed in Section 3.4, some modifications were introduced in the base plant model described in Section 4 in order to simulate the critical events and the additional safety barriers.

In critical scenario 1, a single pulse disturbance was added to signal 1 in Fig. 6 to simulate the critical scenario. The pulse was considered to start 35 min after the beginning of the simulation, and to have a duration of 15 min and an amplitude of 3300 mg_{HCl}/Nm^3, which represents a deviation of 5.5 times the average HCl concentration levels in the flue gas of the reference plant.

As discussed above, a safety barrier consisting in dolomitic lime injection in the furnace was introduced in the model to control the HCl concentration in the flue gas entering the FGT system in the presence of HCl spikes. According to Dal Pozzo et al. (2020), the following correlation can be used to link the dolomitic sorbent feed rate and the corresponding HCl conversion:

$$\chi = \frac{SR^{1.38} - SR}{SR^{1.38} - 1} \tag{9}$$

where χ is the conversion of HCl and SR is the Stochiometric Ratio, representing the ratio between the actual feed rate of dolomitic sorbent and its theoretical demand to achieve full HCl removal according to stoichiometry (Vehlow, 2015). The exponent in Eq. (9) is an empirical parameter derived from tests at WtE facilities (Dal Pozzo et al., 2020). This correlation can be used to obtain the final HCl concentration in the flue gas leaving the furnace after the activation of the dolomitic lime injection system. However, it does not reveal the dynamic of the phenomenon. Therefore, a simplified data-driven approach was followed to obtain the time trend of the HCl concentration in the flue gas after the activation of the safety barrier. Specifically, non-linear least squares were used to fit 4th-order polynomial functions to experimental data. These data consist of 10 experimental runs of dolomitic lime injection performed at different SR values (see Dal Pozzo et al., 2020). The following procedure was used to obtain the optimal fitting:

1. Experimental data were divided into three distinct groups based on their average SR value. Selected SR values are SR = 1, SR = 1.8, and SR = 2.5.
2. Experimental data were scaled in the range (0, 1) through min-max normalization.

$$\widehat{C}_{HCl}(t) = \frac{C_{HCl}(t) - min(C_{HCl}(t))}{\max(C_{HCl}(t)) - \min(C_{HCl}(t))} \tag{10}$$

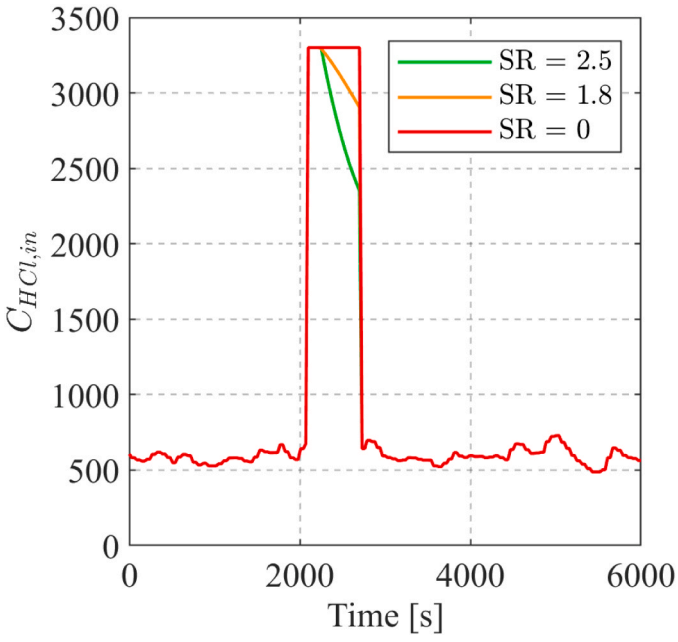

Fig. 9. Effect of the safety barrier considered (dolomitic lime injection) on the HCl concentration in critical event 1. The concentration of HCL considering two different configurations of safety barrier (SR 1.8 and SR 2.5) is compared to the baseline concentration in the absence of safety barriers.

Where $C_{HCl}(t)$ represents the HCl concentration in the flue gas leaving the furnace after the activation of the sorbent injection system, and $\widehat{C}_{HCl}(t)$ indicates the scaled concentration.

3. Scaled experimental data that belong to the same SR group were used to fit 4th-order polynomial functions through non-linear least squares.

$$\widehat{C}_{HCl}(t) = a \bullet t^4 + b \bullet t^3 + c \bullet t^2 + d \bullet t + e \tag{11}$$

where a, b, c, d, and e represent the function parameters.

The fitting procedure led to the parameters shown in Table A1, while the resulting fittings of experimental data is shown in Figure A2 in Appendix 2. Now, the following equations are available:

$$\begin{cases} \dfrac{C_{HCl}(t) - min(C_{HCl}(t))}{max(C_{HCl}(t)) - min(C_{HCl}(t))} = a \bullet t^4 + b \bullet t^3 + c \bullet t^2 + d \bullet t + e \\ \dfrac{SR^{1.38} - SR}{SR^{1.38} - 1} = 1 - \dfrac{C_f}{C_0} \end{cases} \tag{12}$$

where C_f is the final HCl concentration and C_0 is the initial concentration. It is worth noting that the second equation is Eq. (9). Considering that in a simulation SR is user-defined, the parameters a, b, c, d, and e are known. Also, assuming that $C_0 = \max(C_{HCl}(t))$ represents the HCl concentration when the furnace injection system starts and $C_f = \min(C_{HCl}(t))$ indicates the HCl concentration when the injection system stops, Eq. (12) can be used to calculate $C_{HCl}(t)$ and, therefore, to model the barrier dynamics.

Fig. 9 shows the effect of the activation of dolomitic lime injection on critical event 1 (a 15-minute-long spike of HCl). The red curve in the figure (i.e., SR = 0) represents the HCl concentration in the flue gas entering the FGT system during critical scenario 1 when no safety barrier is activated. The orange and green lines show the system behavior after the installation of the safety barrier, which is activated two minutes after the beginning of the peak and stays active until the end of the disturbance. Two different barrier configurations were investigated: SR = 1.8 (orange line) and SR = 2.5 (green line).

With respect to critical event 2, the failure of the screw feeder was simulated as a period of variable duration in which the sorbent mass flow rate (stream 3 in Fig. 6) is set to 0 kg/h. This is achieved by modifying the sorbent mass flow rate as follows:

$$\dot{m}_{sorbent}(t) = \begin{cases} \dot{m}_{sorbent}(t) & if\ t < t_f \ \vee \ t > t_b \\ 0 & if\ t_f \leq t \leq t_b \end{cases} \tag{13}$$

where $t_f = 45$ min indicates the time of failure and t_r represents the time of activation of the backup screw feeder. As mentioned in Section 5.1, in the base case it was assumed that the activation of the backup feeder is manual. A time window of 5 min ($t_b = t_f + 300$ s) seems plausible for operators to acknowledge the alarm, interpret the situation, and take action.

The overall effect of the specific safety barrier identified for this event (automatic activation of the backup feeder) is to reduce the time required to activate the backup screw feeder. This behavior can be simulated by reducing t_b in eq. (13). A response time of 15 s was deemed sufficient for the Safety Instrumented System to activate the backup feeder by plant personnel and instrumentation experts ($t_b = t_f + 15$ s) when the safety barrier is present.

5.3. Simulation of critical scenarios

Two sets of simulations were performed, as mentioned in Section 3.5. The first group of simulations evaluates the response of the original FGT system during critical scenarios (i.e., with no additional safety barrier). The second group of simulations aims to assess the system response after installing the safety barriers.

The results of the simulations of the first critical scenario and safety barrier are shown in Fig. 10a. The red line represents the HCl concentration in the clean gas leaving the original FGT system during the first critical event (i.e., HCl peak). The orange and green lines indicate the response of the system in case of activation of the dolomitic lime injection.

The system performance in the second critical scenario with and without considering the safety barrier is shown in Fig. 10b. Also in this case, the red line represents the response of the original system, while the green line indicates the system response with automatic activation of the backup screw feeder.

5.4. Assessment and comparison of safety barriers

In order to allow the qualitative and quantitative comparison of alternatives, the results of the simulations were used to compute the

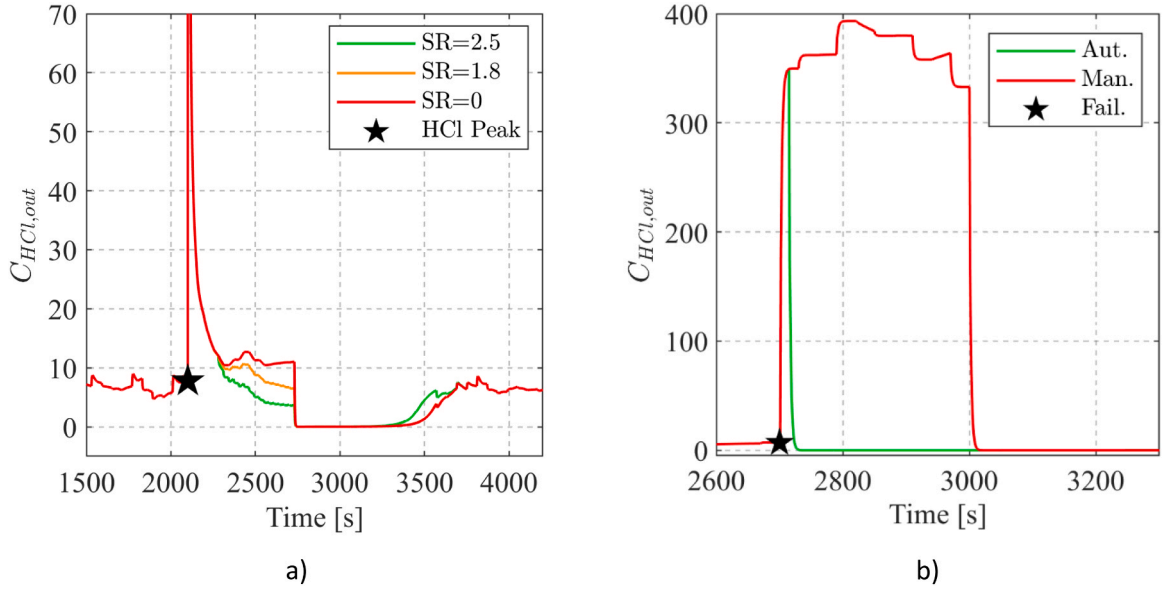

Fig. 10. Simulation of critical scenarios with and without safety barriers: a) critical scenario 1 with or without dolomitic lime injection, b) critical scenario 2 with or without automatic activation of the backup screw feeder.

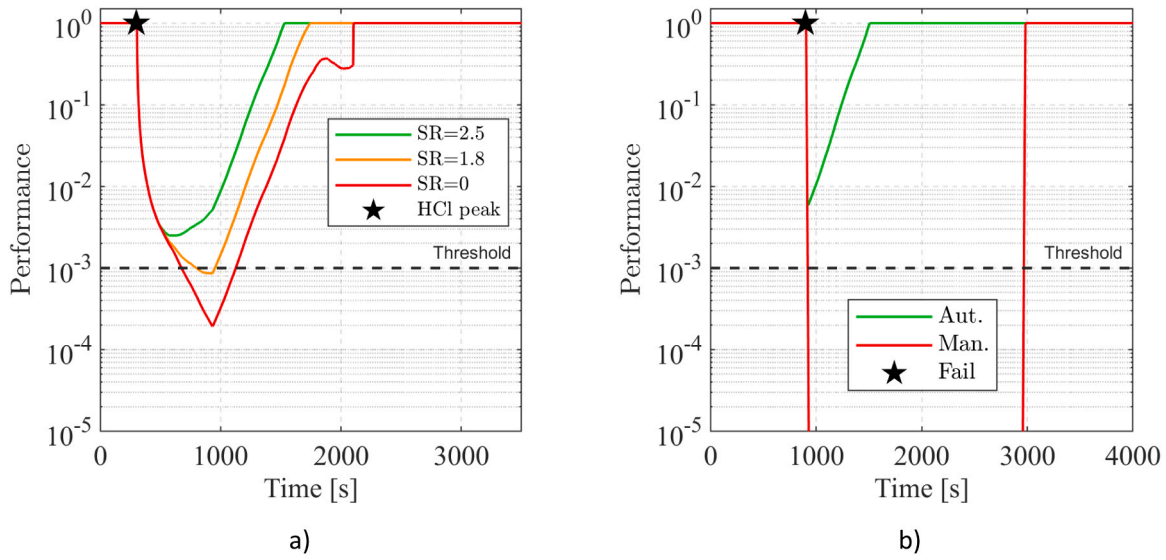

Fig. 11. System performance as defined in Eq. (8) for a) critical scenario 1 with or without dolomitic lime injection and b) critical scenario 2 with or without automatic activation of the backup screw feeder. Dashed threshold line corresponds to ELV HCl concentration. In panel (b), the values of performance for the manual case fall below the lower limit for y-axis was set at 10^{-5} to allow readability.

Table 2
Resilience loss for the two critical scenarios with and without safety barriers.

Critical scenario	Safety barrier	RL [s]
1	No	1651
1	Dolomitic lime injection (SR=1.8)	1302
1	Dolomitic lime injection (SR=2.5)	1103
2	No	2072
2	Automatic backup feeder	487

resilience indicators defined in Section 3.6: the performance metric ($\varphi(t)$) and the Resilience Loss (RL).

The time-trend of the performance indicator for the first critical event and safety barrier is shown in Fig. 11a. The red line represents the performance of the original system, and the orange and green lines indicate the performance after the installation of the dolomitic lime injection.

Similarly, the results of the second critical event and safety barrier are shown in Fig. 11b. It is worth mentioning that in critical event 2 the performance of the original system (i.e., the red curve in Fig. 11b), defined by Eq.(8), drops to 10^{-60}, with HCl concentrations significantly higher the ELVs. In order to increase the readability of the plot in Fig. 11b, the lower limit of the y-axis was set at 10^{-5}. The values calculated for the Resilience Loss in each scenario are summarized in Table 2.

6. Discussion

In several industrial applications, the current practice concerning the optimization of full-scale industrial processes is highly empirical and based on test-runs. However, as discussed above, this approach could hardly be applied to investigate the system performance in the vicinity of emission limits due to the risk of exceeding emission limits during the tests and to the negative consequences related to such events. As shown in Sections 5.3 and 5.4, the use of a digital model combined to hazard identification techniques allowed the identification and dynamic simulation of critical events and, more importantly, the performance assessment of safety barriers. In particular, the results obtained show the possibility of simulating the dynamic behavior of environmentally critical systems with and without safety barriers, providing a quantitative feedback on the increase in the operability, environmental safety and resilience of the system deriving from the installation of such barriers. Thus, the proposed approach can offer to plant managers, control room operators, and safety practitioners a crucial support in the decision-making process for the installation of safety barriers.

When considering the specific results obtained in the case-study, it is clear that in the case of the first critical event identified, as shown in Fig. 11a, the original system cannot withstand the deviations considered. Actually, the performance (red line) decreases rapidly after the critical event and reaches a minimum of $2\bullet10^{-4}$, which indicates that the system could not comply with the ELVs. The performance curves obtained at SR = 1.8 (orange) and SR = 2.5 (green) show that a safety barrier consisting in a dolomitic sorbent injection system in the furnace has the potential to mitigate the first critical scenario. In fact, the minimum performance increases if larger SRs are used. Also, the safety barrier ensures that the minimum performance occurs earlier, which indicates a faster recovery. However, the results also show that a stochiometric ratio equal to 1.8 (orange line) is insufficient to avoid exceeding emission limits. Indeed, the system performance briefly crosses the threshold of $1\bullet10^{-3-3}$ and reaches a minimum of $8.57\bullet10^{-4}$. On the contrary, the system performance obtained with SR equal to 2.5 (green line) reaches a minimum of $5\bullet10^{-3}$, which implies that the emission limit has never been exceeded. This finding confirms that the proposed approach can not only evaluate the dynamic response of safety barriers, but also guide the optimal tuning of their configuration. It should also be remarked that carrying out test-runs at the existing facility to explore system behavior in the conditions addressed would have been hardly feasible, since compliance to ELVs during tests is not granted.

Regarding the second critical scenario, the original system undergoes a complete degradation of performance during the whole critical event (red line in Fig. 11b). On the contrary, the automatic startup of the backup feeder ensures a minimum performance of $6\bullet10^{-3}$, which guarantees compliance with the ELVs.

The analysis of the performance metrics (Fig. 11) shows that the proposed safety barriers can effectively mitigate the critical scenarios considered in the case-study carried out. The Resilience Loss may be used to quantify the improvements brought by the additional safety barriers considered for implementation. Table 2 reveals that the dolomitic lime injection increases the system resilience by 21% (SR = 1.8), and by 33% (SR = 2.5) respectively when considering the first critical scenario. Similarly, the second safety barrier improves system resilience by 76%. It must be stressed these results do not suggest that the second safety barrier should be preferred over the first one. Actually, each safety

barrier is installed to deal with a specific event, which means that the second safety barrier does not affect the first critical scenario and vice versa. Performance comparison of design alternatives should be limited to those referring to the same critical event.

It is also important to mention some limitations of the proposed approach that need to be considered. Firstly, it is evident that the proposed approach, being based on data-driven models, specifically addresses the retrofitting of existing plants, rather than the design of new plants. Nonetheless, even when considering the case-study, the potential relevance of the method emerges, in spite of this limitation. Actually, in the framework of rapidly evolving regulations on emission control worldwide (Huang et al., 2021; Van Caneghem et al., 2019), existing WtE facilities need to increase the performance of their FGT systems in terms of both removal efficiency and reliability.

Secondly, the proposed approach addresses specifically the quantification of the effectiveness of the safety barrier. In addition to effectiveness, the assessment of safety barriers should take into account other criteria, namely response time, availability and level of confidence (de Dianous and Fievez, 2006). The response time, intended as the duration between the deployment of the safety barrier and the complete achievement of its safety function (de Dianous and Fievez, 2006), can be estimated from the results of the simulations (see again Fig. 11). The time between the detection of the ELV exceedance and the activation of the barrier is a required input of the simulations and, as discussed in Section 5.2, it can be obtained from tests (as in the case of dolomitic lime injection) or from operating experience (as in the case of the backup screw feeder). The time between the activation of the barrier and the full achievement of its safety function is an output of the simulations, as they are dynamic by nature and trace the evolution of barrier effectiveness over time. Conversely, aspects related to the level of confidence and the availability of the barrier are not assessed in the proposed approach, since they are associated with inherent properties and maintenance strategies of the barrier components and not with the effect of the safety barrier on the functionality of the FGT system, which is the key mechanism addressed by the simulations.

Thirdly, in the proposed approach, the evaluation of safety barriers is approached solely from an environmental perspective, while economic aspects have been disregarded in the case study. This choice aimed to demonstrate the feasibility and usefulness of the approach without introducing additional complexity. However, economic aspects must be considered when evaluating alternatives. For example, the user may combine performance and resilience assessment with cost-benefit analysis or more comprehensive techniques such as Life Cycle Assessment (LCA) (International Organization for Standardization, 2006). Alternatively, further studies may focus on improving the performance metric proposed in Eq. (8) to consider the costs associated with a particular process configuration.

Lastly, in the case-study a single barrier was considered for each critical event. On the one hand, a more realistic approach would be to consider and compare different safety barriers, from the safety, environmental and economic perspective. On the other hand, considering a single barrier provides a straightforward application of the methodology to different critical scenarios. Thus, since the intent of the case study is to provide a full-scale notional application of the methodology, the latter approach was privileged. Nevertheless, the approach developed and the specific models may be used as well to address the comparison and selection of safety barriers in a more comprehensive decision-making framework.

All in all, the application of the methodology demonstrated the possibilities arising from the integration between hazard identification techniques (e.g., HazOp and Bow-Tie analysis) and advanced simulation tools (i.e., dynamic modeling and resilience analysis) in the context of environmental risk management. The proposed framework is flexible and different choices in terms of both risk identification and process modeling can be adopted, also depending on the characteristics of the reference system and the related data availability.

Moreover, the analysis of the case study suggests that the dynamic modeling of critical events and evaluation of safety barriers through resilience analysis offers an interesting opportunity to improve environmental risk management. The approach goes beyond the static view of safety barriers (i.e., effective-not effective, and characterized by a context-independent Probability of Failure) towards a dynamic vision of the risk, where the effectiveness of safety barriers is closely linked to the dynamics of the underlying phenomena. The methodology fits perfectly in a Dynamic Risk Management framework since it is inherently updatable and can be reiterated to account for changes in the environment (e.g., changes in process conditions or plant layout) (Grøtan and Paltrinieri, 2016) and to incorporate new information as they become available (e.g., considering new critical events as more knowledge is accessible) (Paltrinieri et al., 2014).

7. Conclusions

The approach described in this study offers a comprehensive and structured framework for the dynamic evaluation of safety barriers in environmentally critical facilities based on digital modelling. The method is based on a pre-defined flowcharts of activities, covering most of the risk management phases, from the identification of critical scenarios to the evaluation of the system response. In addition, the method is sufficiently generic to allow some flexibility (e.g., with respect to modeling techniques and tools) in order to be adapted to diverse needs. The approach has several advantages and novelty elements, such as the focus on environmental risk management from a safety engineering perspective (which is often disregarded in the literature) and the integration between traditional risk management techniques and modern data-driven models, which allows the definition and simulation of critical scenarios and safety barriers that would be impossible to evaluate through first-principles or field tests. Furthermore, the methodology requires a relatively small set of data, which is often promptly available in most gas treatment facilities. In addition, the use of resilience analysis for the dynamic evaluation of safety barriers and the intrinsic updatability of the approach are further elements of novelty that contribute to dynamic risk management. The method has been tested on a full-scale real life industrial case study to demonstrate its feasibility and effectiveness. The results – which appear informative, yet easy to interpret – allow qualitative and quantitative evaluation and comparison of safety barriers. In the context of growing attention to environmental issues and widespread digitalization of production processes, this study suggests that data-driven models may effectively support traditional risk management approaches to improve environmental safety and accomplish tasks that are impractical or impossible to perform through first principles.

Declaration of Competing Interest

The authors declare that they have no known competing financial interests or personal relationships that could have appeared to influence the work reported in this paper.

Appendix 1. Results of the HazOp analysis

The full results of the HazOp Analysis are condensed in the bow-tie diagram below.

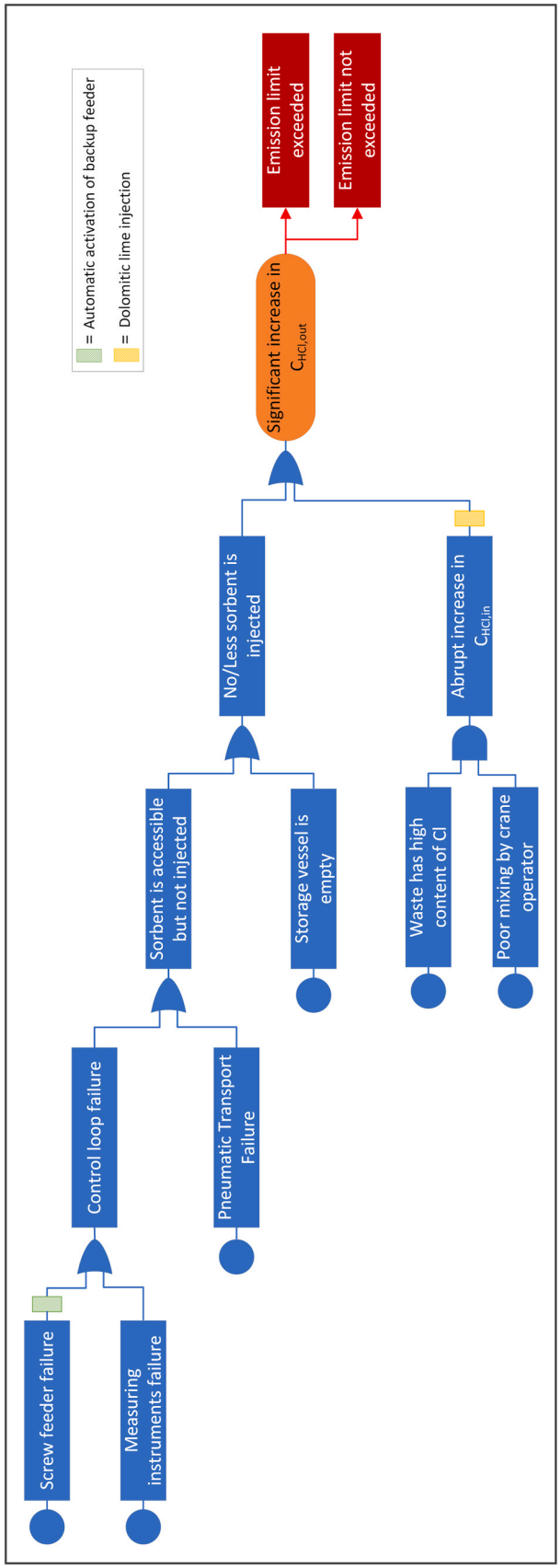

Fig A1. Complete bow-tie diagram for the reference system.

Appendix 2. Supporting information on furnace sorbent injection

Table A1
Fitting parameters for different SR groups.

Group	*a*	*b*	*c*	*d*	*e*
SR∼1	-3.09×10^{-7}	5.99×10^{-5}	-2.46×10^{-3}	-9.71×10^{-4}	9.83×10^{-1}
SR∼1.8	-1.68×10^{-6}	1.33×10^{-4}	-2.50×10^{-3}	-3.16×10^{-2}	1.01×10^{0}
SR∼2.5	-4.41×10^{-7}	-5.08×10^{-5}	5.60×10^{-3}	-1.37×10^{-1}	1.07×10^{0}

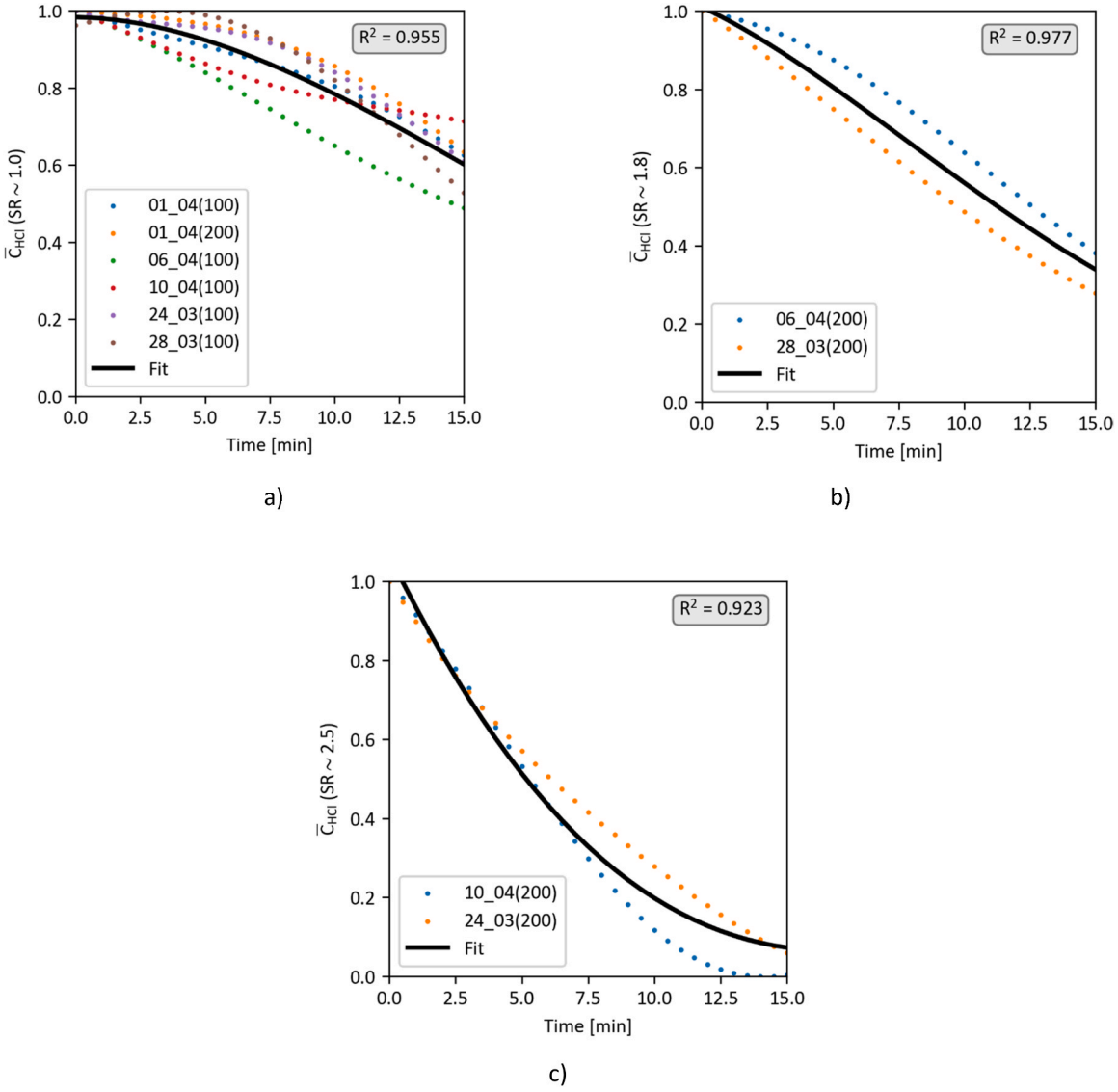

Fig A2. Experimental data and fitting curves for SR∼1 (a), SR∼1.8 (b), SR∼2.5 (c). Experimental runs are named xx_yy(zzz), where xx represents the day of collection, yy indicates the month, and zzz indicates the dolomitic sorbent feed rate in kg/h. The coefficient of determination of the fitting functions (R^2) is displayed in the upper right corner.

Appendix C. Supporting information

Supplementary data associated with this article can be found in the online version at doi:10.1016/j.psep.2023.11.021.

References

Antonioni, G., Dal Pozzo, A., Guglielmi, D., Tugnoli, A., Cozzani, V., 2016. Enhanced modelling of heterogeneous gas–solid reactions in acid gas removal dry processes. Chem. Eng. Sci. 148, 140–154. https://doi.org/10.1016/j.ces.2016.03.009.

Argenti, F., Landucci, G., Cozzani, V., Reniers, G., 2017. A study on the performance assessment of anti-terrorism physical protection systems in chemical plants. Saf. Sci. 94, 181–196. https://doi.org/10.1016/j.ssci.2016.11.022.

Bacci Di Capaci, R., Pannocchia, G., Pozzo, A.D., Antonioni, G., Cozzani, V., 2022. Data-driven models for advanced control of acid gas treatment in waste-to-energy plants. IFAC-Pap. 55, 869–874. https://doi.org/10.1016/j.ifacol.2022.07.554.

Bai, Y., Wu, J., Yuan, S., Reniers, G., Yang, M., Cai, J., 2022. Dynamic resilience assessment and emergency strategy optimization of natural gas compartments in utility tunnels. Process Saf. Environ. Prot. 165, 114–125. https://doi.org/10.1016/j.psep.2022.07.008.

Bergström, J., van Winsen, R., Henriqson, E., 2015. On the rationale of resilience in the domain of safety: a literature review. Reliab. Eng. Syst. Saf. 141, 131–141. https://doi.org/10.1016/j.ress.2015.03.008.

Beylot, A., Hochar, A., Michel, P., Descat, M., Ménard, Y., Villeneuve, J., 2018. Municipal solid waste incineration in france: an overview of air pollution control techniques, emissions, and energy efficiency. J. Ind. Ecol. 22, 1016–1026. https://doi.org/10.1111/jiec.12701.

Biganzoli, L., Racanella, G., Marras, R., Rigamonti, L., 2015. High temperature abatement of acid gases from waste incineration. Part II: Comparative life cycle assessment study. Waste Manag 35, 127–134. https://doi.org/10.1016/j.wasman.2014.10.021.

Box, G.E.P., Jenkins, G.M., Reinsel, G.C., Ljung, G.M., 2015. Time series analysis: forecasting and control. Wiley Series in Probability and Statistics. Wiley.

Bubbico, R., Lee, S., Moscati, D., Paltrinieri, N., 2020. Dynamic assessment of safety barriers preventing escalation in offshore Oil&Gas. Saf. Sci. 121, 319–330. https://doi.org/10.1016/j.ssci.2019.09.011.

Bucelli, M., Landucci, G., Haugen, S., Paltrinieri, N., Cozzani, V., 2018. Assessment of safety barriers for the prevention of cascading events in oil and gas offshore installations operating in harsh environment. Ocean Eng. 158, 171–185. https://doi.org/10.1016/j.oceaneng.2018.02.046.

CCPS, Energy Institute, 2018. Bow ties in risk management. Bow Ties in Risk Management. Wiley. https://doi.org/10.1002/9781119490357.

Chibante, V.G., Fonseca, A.M., Salcedo, R.R., 2010. Modeling dry-scrubbing of gaseous HCl with hydrated lime in cyclones with and without recirculation. J. Hazard. Mater. 178, 469–482. https://doi.org/10.1016/j.jhazmat.2010.01.106.

Daintith, J., Wright, E., 2008. A Dictionary of Computing. Oxford University Press. https://doi.org/10.1093/acref/9780199234004.001.0001.

Dal Pozzo, A., Capecci, S., Cozzani, V., 2023b. Techno-economic impact of lower emission standards for waste-to-energy acid gas emissions. Waste Manag.

Dal Pozzo, A., Lucquiaud, M., De Greef, Johan, 2023c. Research and innovation needs for the Waste-to-Energy sector towards a net-zero circular economy. Energies.

Dal Pozzo, A., Antonioni, G., Guglielmi, D., Stramigioli, C., Cozzani, V., 2016. Comparison of alternative flue gas dry treatment technologies in waste-to-energy processes. Waste Manag 51, 81–90. https://doi.org/10.1016/j.wasman.2016.02.029.

Dal Pozzo, A., Guglielmi, D., Antonioni, G., Tugnoli, A., 2018a. Environmental and economic performance assessment of alternative acid gas removal technologies for waste-to-energy plants. Sustain. Prod. Consum 16, 202–215. https://doi.org/10.1016/j.spc.2018.08.004.

Dal Pozzo, A., Moricone, R., Antonioni, G., Tugnoli, A., Cozzani, V., 2018b. Hydrogen chloride removal from flue gas by low-temperature reaction with calcium hydroxide. Energy Fuels 32, 747–756. https://doi.org/10.1021/acs.energyfuels.7b03292.

Dal Pozzo, A., Lazazzara, L., Antonioni, G., Cozzani, V., 2020. Techno-economic performance of HCl and SO2 removal in waste-to-energy plants by furnace direct sorbent injection. J. Hazard. Mater. 394, 122518 https://doi.org/10.1016/j.jhazmat.2020.122518.

Dal Pozzo, A., Muratori, G., Antonioni, G., Cozzani, V., 2021. Economic and environmental benefits by improved process control strategies in HCl removal from waste-to-energy flue gas. Waste Manag. 125, 303–315. https://doi.org/10.1016/j.wasman.2021.02.059.

Dal Pozzo, A., Abagnato, S., Cozzani, V., 2023a. Assessment of cross-media effects deriving from the application of lower emission standards for acid pollutants in waste-to-energy plants. Sci. Total Environ. 856, 159159 https://doi.org/10.1016/j.scitotenv.2022.159159.

Delvosalle, C., Fievez, C., Pipart, A., Debray, B., 2006. ARAMIS project: a comprehensive methodology for the identification of reference accident scenarios in process industries. J. Hazard. Mater. 130, 200–219. https://doi.org/10.1016/j.jhazmat.2005.07.005.

de Dianous, V., Fievez, C., 2006. ARAMIS project: a more explicit demonstration of risk control through the use of bow–tie diagrams and the evaluation of safety barrier performance. J. Hazard. Mater. 130, 220–233. https://doi.org/10.1016/j.jhazmat.2005.07.010.

Emmert-Streib, F., Dehmer, M., 2019. Evaluation of regression models: model assessment, model selection and generalization error. Mach. Learn. Knowl. Extr. 1, 521–551. https://doi.org/10.3390/make1010032.

European Commission, 2019. Best Available Techniques (BAT) Reference Document for Waste Incineration, EUR 29971 EN. https://doi.org/10.2760/761437.

European Commission, 2020. Best Available Techniques (BAT) reference document for waste incineration: Industrial Emissions Directive 2010/75/EU (Integrated Pollution Prevention and Control). Publications Office. https://doi.org/doi/10.2760/761437.

Grøtan, T.O., Paltrinieri, N., 2016. Chapter 20 - Dynamic Risk Management in the Perspective of a Resilient System. In: Paltrinieri, Nicola, Khan, F. (Eds.), Dynamic Risk Analysis in the Chemical and Petroleum Industry. Butterworth-Heinemann, pp. 245–257. https://doi.org/10.1016/B978-0-12-803765-2.00020-2.

Han, Y., Zhen, X., Huang, Y., Vinnem, J.E., 2019. Integrated methodology for determination of preventive maintenance interval of safety barriers on offshore installations. Process Saf. Environ. Prot. 132, 313–324. https://doi.org/10.1016/j.psep.2019.09.035.

Hokstada, P., Øien, K., Reinertsen, R., 1998. Recommendations on the use of expert judgment in safety and reliability engineering studies. Two offshore case studies. Reliab. Eng. Syst. Saf. 61, 65–76. https://doi.org/10.1016/S0951-8320(97)00084-7.

Hollnagel, E., Paries, J., Woods David, D., Wreathall, J., 2010. Resilience Engineering in Practice: A Guidebook, Ashgate Studies in Resilience Engineering. Ashgate Publishing.

Hollnagel, E., Pariès, J., Woods, D.D., Wreathall, J., 2011. Resilience Engineering in Practice: A Guidebook, 1st ed. Ashgate, Farnham, England.

Hosseini, S., Barker, K., Ramirez-Marquez, J.E., 2016. A review of definitions and measures of system resilience. Reliab. Eng. Syst. Saf. 145, 47–61. https://doi.org/10.1016/j.ress.2015.08.006.

Huang, W., Li, H., Fan, H., Qian, Y., 2021. Causation mechanism analysis of excess emission of flue gas pollutants from municipal solid waste incineration power plants by employing the Fault Tree combined with Bayesian Network: A case study in Dongguan. J. Clean. Prod. 327, 129533 https://doi.org/10.1016/j.jclepro.2021.129533.

International Organization for Standardization, 2006. Environmental management — Life cycle assessment — Principles and framework, ISO 14040:2006(E). Geneva, CH.

International Organization for Standardization, 2018. Risk management - Guidelines, ISO 31000:2018. Geneva, CH.

International Organization for Standardization, 2019. Risk management - Risk assessment techniques, IEC 31010:2019. Geneva, CH.

Khan, F., Rathnayaka, S., Ahmed, S., 2015. Methods and models in process safety and risk management: Past, present and future. Process Saf. Environ. Prot. 98, 116–147. https://doi.org/10.1016/j.psep.2015.07.005.

Khan, F., Hashemi, S.J., Paltrinieri, N., Amyotte, P., Cozzani, V., Reniers, G., 2016. Dynamic risk management: a contemporary approach to process safety management. Curr. Opin. Chem. Eng. 14, 9–17. https://doi.org/10.1016/j.coche.2016.07.006.

Knight, J.C., 2002. Safety critical systems: challenges and directions, in: Proceedings of the 24th International Conference on Software Engineering. ICSE 2002. pp. 547–550.

Kockmann, N., 2019. Digital methods and tools for chemical equipment and plants. React. Chem. Eng. 4, 1522–1529. https://doi.org/10.1039/C9RE00017H.

Kotu, V., Deshpande, B., 2019. Chapter 12 - time series forecasting. In: Kotu, V., Deshpande, B. (Eds.), Data Science (Second Edition). Morgan Kaufmann, pp. 395–445. https://doi.org/10.1016/B978-0-12-814761-0.00012-5.

Landucci, G., Argenti, F., Tugnoli, A., Cozzani, V., 2015. Quantitative assessment of safety barrier performance in the prevention of domino scenarios triggered by fire. Reliab. Eng. Syst. Saf. 143, 30–43. https://doi.org/10.1016/j.ress.2015.03.023.

Leveson, N., Dulac, N., Zipkin, D., Cutcher-Gershenfeld, J., Carroll, J., Barrett, B., 2006. Chapter 8 - Engineering Resilience into Safety-Critical Systems. In: Hollnagel, E., Woods, D.D., Leveson, N. (Eds.), Resilience Engineering Concepts and Precepts. Ashgate Publishing Limited. https://doi.org/10.1201/9781315605685.

Liu, Y., 2020. Safety barriers: Research advances and new thoughts on theory, engineering and management. J. Loss Prev. Process Ind. 67, 104260 https://doi.org/10.1016/j.jlp.2020.104260.

Ljung, L., 1999. System identification: theory for the user. Prentice Hall information and system sciences series. Prentice Hall PTR,.

Ljung, L., 2010. Perspectives on system identification. Annu. Rev. Control 34, 1–12. https://doi.org/10.1016/j.arcontrol.2009.12.001.

Magnanelli, E., Tranås, O.L., Carlsson, P., Mosby, J., Becidan, M., 2020. Dynamic modeling of municipal solid waste incineration. Energy 209, 118426. https://doi.org/10.1016/j.energy.2020.118426.

Mannan, S., 2005. Hazard Identification. In: Mannan, S. (Ed.), Lees' Loss Prevention in the Process Industries. Elsevier, Burlington, pp. 8/1–8/79. https://doi.org/10.1016/B978-075067555-0.50096-7.

Maurya, A., Kumar, D., 2020. Reliability of safety-critical systems: a state-of-the-art review. Qual. Reliab. Eng. Int. 36, 2547–2568. https://doi.org/10.1002/qre.2715.

Misuri, A., Landucci, G., Cozzani, V., 2020. Assessment of safety barrier performance in Natech scenarios. Reliab. Eng. Syst. Saf. 193, 106597 https://doi.org/10.1016/j.ress.2019.106597.

Misuri, A., Landucci, G., Cozzani, V., 2021. Assessment of risk modification due to safety barrier performance degradation in Natech events. Reliab. Eng. Syst. Saf. 212, 107634 https://doi.org/10.1016/j.ress.2021.107634.

Paltrinieri, N., Khan, F.I., 2020. Dynamic. risk Anal. 35–60. https://doi.org/10.1016/bs.mcps.2020.04.001.

Paltrinieri, N., Khan, F., Amyotte, P., Cozzani, V., 2014. Dynamic approach to risk management: Application to the Hoeganaes metal dust accidents. Process Saf. Environ. Prot. 92, 669–679. https://doi.org/10.1016/j.psep.2013.11.008.

Patriarca, R., Bergström, J., Di Gravio, G., Costantino, F., 2018. Resilience engineering: Current status of the research and future challenges. Saf. Sci. 102, 79–100. https://doi.org/10.1016/j.ssci.2017.10.005.

Pozzo, A.D., Giannella, M., Antonioni, G., Cozzani, V., 2018. Optimization of the economic and environmental profile of HCl removal in a municipal solid waste incinerator through historical data analysis. Chem. Eng. Trans. 67, 463–468. https://doi.org/10.3303/CET1867078.

Raschka, S., 2018. Model evaluation, model selection, and algorithm selection. Mach. Learn. https://doi.org/10.48550/ARXIV.1811.12808.

Sarvestani, K., Ahmadi, O., Mortazavi, S.B., Mahabadi, H.A., 2021. Development of a predictive accident model for dynamic risk assessment of propane storage tanks. Process Saf. Environ. Prot. 148, 1217–1232. https://doi.org/10.1016/j.psep.2021.02.018.

Sklet, S., 2006. Safety barriers: Definition, classification, and performance. J. Loss Prev. Process Ind. 19, 494–506. https://doi.org/10.1016/j.jlp.2005.12.004.

Sun, H., Wang, H., Yang, M., Reniers, G., 2021. Resilience-based approach to safety barrier performance assessment in process facilities. J. Loss Prev. Process Ind. 73, 104599 https://doi.org/10.1016/j.jlp.2021.104599.

Thieme, C.A., Utne, I.B., 2017. Safety performance monitoring of autonomous marine systems. Reliab. Eng. Syst. Saf. 159, 264–275. https://doi.org/10.1016/j.ress.2016.11.024.

Torres, J.F., Hadjout, D., Sebaa, A., Martínez-Álvarez, F., Troncoso, A., 2020. Deep Learning for Time Series Forecasting: A Survey. Big Data 9, 3–21. https://doi.org/10.1089/big.2020.0159.

Tran, H.T., Balchanos, M., Domerçant, J.C., Mavris, D.N., 2017. A framework for the quantitative assessment of performance-based system resilience. Reliab. Eng. Syst. Saf. 158, 73–84. https://doi.org/10.1016/j.ress.2016.10.014.

V. De Dianous D. Hourtolou E. Bernuchon ARAMIS D1C – APPENDIX 2004 9.

Van Caneghem, J., Van Acker, K., De Greef, J., Wauters, G., Vandecasteele, C., 2019. Waste-to-energy is compatible and complementary with recycling in the circular economy. Clean. Technol. Environ. Policy 21, 925–939. https://doi.org/10.1007/s10098-019-01686-0.

Vehlow, J., 2015. Air pollution control systems in WtE units: An overview. Waste Manag 37, 58–74. https://doi.org/10.1016/j.wasman.2014.05.025.

Villa, V., Paltrinieri, N., Khan, F., Cozzani, V., 2016. Towards dynamic risk analysis: A review of the risk assessment approach and its limitations in the chemical process industry. Saf. Sci. 89, 77–93. https://doi.org/10.1016/j.ssci.2016.06.002.

Wang, Q., Ma, Y., Zhao, K., Tian, Y., 2022. A Comprehensive Survey of Loss Functions in Machine Learning. Ann. Data Sci. 9, 187–212. https://doi.org/10.1007/s40745-020-00253-5.

Yarveisy, R., Gao, C., Khan, F., 2020. A simple yet robust resilience assessment metrics. Reliab. Eng. Syst. Saf. 197, 106810 https://doi.org/10.1016/j.ress.2020.106810.

Zeng, T., Chen, G., Yang, Y., Chen, P., Reniers, G., 2020. Developing an advanced dynamic risk analysis method for fire-related domino effects. Process Saf. Environ. Prot. 134, 149–160. https://doi.org/10.1016/j.psep.2019.11.029.